

DEVELOPMENT OF GRAPHICAL USER  
INTERFACE (GUI) FOR BEARING FAULT  
DETECTION

SYAHIDAH NAFISA BTE ABDUL MALIK

BACHELOR OF ENGINEERING  
UNIVERSITI MALAYSIA PAHANG

DEVELOPMENT OF GRAPHICAL USER INTERFACE (GUI) FOR BEARING  
FAULT DETECTION

SYAHIDAH NAFISA BTE ABDUL MALIK

Thesis submitted in fulfilment of the requirements  
for the award of the degree of Bachelor of Mechanical Engineering

Faculty of Mechanical Engineering  
UNIVERSITI MALAYSIA PAHANG

JUNE 2013

UNIVERSITI MALAYSIA PAHANG

**BORANG PENGESAHAN STATUS TESIS♦**

JUDUL: **DEVELOPMENT OF GRAPHICAL USER INTERFACE  
(GUI) FOR BEARING FAULT DETECTION**  
SESI PENGAJIAN: 2010/2013

Saya SYAHIDAH NAFISA BTE ABDUL MALIK (890114-04-5272)  
(HURUF BESAR)

mengaku membenarkan tesis (Sarjana Muda/~~Sarjana~~ /~~Doktor Falsafah~~)\* ini disimpan di Perpustakaan dengan syarat-syarat kegunaan seperti berikut:

1. Tesis adalah hakmilik Universiti Malaysia Pahang (UMP).
2. Perpustakaan dibenarkan membuat salinan untuk tujuan pengajian sahaja.
3. Perpustakaan dibenarkan membuat salinan tesis ini sebagai bahan pertukaran antara institusi pengajian tinggi.
4. \*\*Sila tandakan ( √ )

**SULIT**

(Mengandungi maklumat yang berdarjah keselamatan atau kepentingan Malaysia seperti yang termaktub di dalam AKTA RAHSIA RASMI 1972)

**TERHAD**

(Mengandungi maklumat TERHAD yang telah ditentukan oleh organisasi/badan di mana penyelidikan dijalankan)

**TIDAK TERHAD**

Disahkan oleh:

\_\_\_\_\_  
(TANDATANGAN PENULIS)

\_\_\_\_\_  
(TANDATANGAN PENYELIA)

Alamat Tetap:

**NO. 465-3, KM 16**  
**KAMPUNG KRUBONG**  
**75250 MELAKA**  
**MELAKA**

**MOHAMAD ZAIRI BIN BAHAROM**  
( Nama Penyelia )

Tarikh: **27 JUN 2013**

Tarikh: : **27 JUN 2013**

- CATATAN:
- \* Potong yang tidak berkenaan.
  - \*\* Jika tesis ini SULIT atau TERHAD, sila lampirkan surat daripada pihak berkuasa/organisasi berkenaan dengan menyatakan sekali tempoh tesis ini perlu dikelaskan sebagai atau TERHAD.
  - ♦ Tesis dimaksudkan sebagai tesis bagi Ijazah doktor Falsafah dan Sarjana secara Penyelidikan, atau disertasi bagi pengajian secara kerja kursus dan penyelidikan, atau Laporan Projek Sarjana Muda (PSM).

**UNIVERSITI MALAYSIA PAHANG**  
**FACULTY OF MECHANICAL ENGINEERING**

I certify that the project entitled “Development of Graphical User Interface (GUI) For Bearing Fault Detection” is written by Syahidah Nafisa bte Abdul Malik. I have examined the final copy of this project and in my opinion it is fully adequate in terms of language standard and report formatting requirement for the award of the degree of Bachelor of Engineering. I herewith recommend that it be accepted in partial fulfilment of the requirements for the degree of Bachelor of Mechanical Engineering.

ABDUL GHAFFAR BIN ABDUL RAHMAN

Examiner

Signature

## **SUPERVISOR'S DECLARATION**

I hereby declare that I have checked this project and in my opinion this project is satisfactory in terms of scope and quality for the award of the degree of Bachelor's Degree of Mechanical Engineering.

Signature : .....

Name of Supervisor : MOHAMAD ZAIRI B BAHAROM

Position : FINAL YEAR PROJECT SUPERVISOR

Date : 27 JUNE 2013

## STUDENT'S DECLARATION

I hereby declare that the work in this thesis entitles “Development of Graphical User Interface for Bearing Fault Detection” is the result of my own research except as cited in the references. The thesis has not been accepted for any bachelor's degree concurrently submitted in candidature of any other degrees.

Signature : .....

Name : SYAHIDAH NAFISA BTE ABDUL MALIK

ID Number : MA 10093

Date : 27 JUNE 2013

## ACKNOWLEDGEMNT

In the name of Allah S.W.T the Most Beneficent and the Most Merciful. The deepest sense of gratitude to the Almighty for the strength and ability to complete this project. Infinite thanks I brace upon Him.

I am grateful and would like to express my sincere gratitude to my supervisors Mr. Mohamad Zairi b Baharom and Mr. Che Ku Eddy Nizwan b Che Ku Husin for providing this interesting and exciting topic and then providing his guidance, assistance and encouragement throughout the duration of the project. I appreciate his consistent support from the first day I applied to graduate program to these concluding moments. I am also thankful to Advances Structural Integrity & Vibration Research (ASiVR) Focus Group for giving me the advice and related comments and critics on my project to the extent of its completion.

Sincere thanks to all staff of the Mechanical Engineering Department, UMP, who helped me in many ways and providing equipment and information sources that assisted my studies and projects.

To all my committee members, thanks for the comments and suggestions given which is crucial for the successful completion of this study.

Special thanks to my lovely parents for their support, love, dream and sacrifice throughout my life. I would like to appreciate their devotion, support and faith in my ability to attain my goals.

Finally to individuals who was involved either directly nor indirectly in succession of this thesis. Indeed I could never adequately express my indebtedness to all of them. Thank you.

*Specially dedicated to my beloved family and those who have  
Encourage and always be with me during hard times  
And inspired me throughout my journey of learning*



## ABSTRACT

Rolling element bearing has vast domestic and the vital parts in any rotating machinery. Appropriate function of these appliances depends on the smooth operation of the bearings. Failure of this particular part can affect the machinery performance and in time will cause major failure to the machinery. Result of various studies shows that bearing problems account for over 40% of all machine failures. Due to the crucial problem, online monitoring has become an alternative in preventive maintenance. The objective of this project is to develop software with signal processing tools to detect defect features in mechanical signal of the bearing. Five set of bearing were tested with one of them remains in good condition while the other four has its own type of defects. The data for good bearing were used as baseline data to compare with the defected ones. The data consist with three different speed rotation which are 287, 1466, and 2664 rpm. Then analyzed by using Continuous Wavelet Transform (CWT). From there, it is further analyse using wavelet coefficient for each level of decomposition from CWT method. From the result generated, Fast Fourier Transform (FFT) and wavelet coefficient plays an important role in supporting result analyzed by using CWT that will be used on Graphical User Interface (GUI) software in MATLAB. A system or data with low wavelet coefficient compare to the good condition wavelet coefficient will clearly state as in good condition bearing while the defect features still may be recovered by calculating the wavelet coefficient for each level of decomposition in CWT method. If the wavelet coefficient of data is higher than the good bearing, it proves that the defect occurred on that bearing. The GUI will display the result of the CWT process by displaying condition of the bearing either in good condition or not. Finally, the CWT method also proves to be an effective method for online condition monitoring tool with GUI software. Future research should be detecting type of the defect features based on statistical tool.

## ABSTRAK

Galas mempunyai aplikasi domestik dan penting terdapat di dalam jentera berputar. Fungsi peralatan ini bergantung kepada kelancaran gelas sendiri. Kegagalan bahagian ini tertentu boleh menjejaskan prestasi jentera dan dalam masa yang sama, ia akan menyebabkan kegagalan utama kepada jentera. Hasil daripada pelbagai kajian, ia menunjukkan bahawa masalah gelas menyumbang lebih 40% daripada kebanyakan kegagalan mesin. Oleh kerana masalah yang serius, pemantauan dalam talian telah menjadi alternatif bagi penyelenggaraan servis pencegahan mesin. Objektif projek ini adalah untuk membina perisian dengan alat pemprosesan isyarat untuk mengesan ciri-ciri kecacatan dalam isyarat mekanikal pada gelas. Lima set gelas telah diuji dengan salah satu daripada gelas tersebut berada dalam keadaan yang baik, manakala empat yang lain mempunyai berlainan kecacatan. Data untuk gelas yang baik telah digunakan sebagai penanda aras untuk dibandingkan dengan data-data gelas yang rosak. Data tersebut terdiri daripada tiga kelajuan putaran mesin yang berbeza iaitu 287, 1466, dan 2664 putaran per minut. Data ini akan dianalisis dengan menggunakan kaedah *Continous Wavelet Transform (CWT)*. Kemudian, data akan dianalisis menggunakan *Wavelet Coefficient* untuk setiap peringkat penguraian di dalam kaedah CWT. Dari keputusan yang diperolehi, *Fast Fourier Transform (FFT)* dan *wavelet coefficient* memainkan peranan penting dalam analisa CWT dimana keputusan itu akan digunakan pada perisian antara muka grafik pengguna di dalam perisian *MATLAB*. Setiap data yang mempunyai *wavelet coefficient* yang rendah berbanding dengan *wavelet coefficient* gelas rujukan, gelas tersebut berada dalam keadaan yang baik, manakala kecacatan masih boleh dikenalpasti dengan mengira *wavelet coefficient* bagi setiap peringkat penguraian yang digunakan dalam kaedah CWT. Jika *wavelet coefficient* data adalah lebih tinggi daripada *wavelet coefficient* gelas yang baik, ia membuktikan bahawa kecacatan telah berlaku pada gelas tersebut. GUI akan memaparkan hasil daripada proses CWT dengan menyatakan bahawa keadaan gelas sama ada gelas tersebut berada dalam keadaan baik atau tidak. Kesimpulannya, kaedah CWT membuktikan bahawa ia merupakan salah satu kaedah yang berkesan bagi mengenalpasti kehadiran kecacatan gelas dalam talian dengan menggunakan alat pemantauan daripada perisian GUI. Kajian masa depan boleh dilaksanakan dengan mengesan jenis-jenis kecacatan pada gelas tersebut.

## TABLE OF CONTENTS

		<b>Page</b>
<b>EXAMINER’S DECLARATION</b>		iv
<b>SUPERVISOR’S DECLARATION</b>		v
<b>STUDENT’S DECLARATION</b>		vi
<b>ACKNOWLEDGEMENTS</b>		vii
<b>DEDICATION</b>		viii
<b>ABSTRACT</b>		ix
<b>ABSTRAK</b>		x
<b>TABLE OF CONTENTS</b>		xi
<b>LIST OF TABLES</b>		xiv
<b>LIST OF FIGURES</b>		xv
<b>LIST OF SYMBOLS</b>		xvii
<b>LIST OF ABBREVIATIONS</b>		xviii
<b>CHAPTER 1</b>	<b>INTRODUCTION</b>	
1.0	Introduction	1
1.1	Project Background	1
1.2	Problem Statement	2
1.3	Objectives	3
1.4	Project scopes	3
1.5	Project Flow Chart	3
1.6	Thesis Overview	7
<b>CHAPTER 2</b>	<b>LITERATURE REVIEW</b>	
2.0	Introduction	8
2.1	Bearing	8
	2.1.1 Types of bearing defects	9
2.2	Signal Analysis	13
	2.2.1 Frequency Domain Analysis	13

	2.2.2	Time Domain Analysis	15
	2.3	Bearing Fault Detection	19
	2.4	Condition Monitoring	21
	2.5	Continuous Wavelet Transform	22
	2.6	Graphical User Interface	25
<b>CHAPTER 3</b>		<b>METHODOLOGY</b>	
	3.0	Introduction	27
	3.1	Data Processing	27
	3.1.1	Continuous Wavelet Transform	27
	3.2	Development of Graphical User Interface	30
<b>CHAPTER 4</b>		<b>RESULT AND DISCUSSION</b>	
	4.0	Introduction	34
	4.1	Data	34
	4.2	Scalogram Result	37
	4.3	Wavelet Coefficient Analysis	46
	4.3.1	Wavelet coefficient for 287 rpm	46
	4.3.2	Wavelet coefficient for 1466 rpm	48
	4.3.3	Wavelet coefficient for 2664 rpm	49
	4.4	Graphical User Interface	55
<b>CHAPTER 5</b>		<b>CONCLUSION AND RECOMMENDATION</b>	
	5.1	Conclusion	58
	5.2	Recommendation	59
<b>REFERENCES</b>			60

**APPENDICES**

A	Continuous Wavelet Transform MATLAB Coding	62
---	--	----

**LIST OF TABLES**

<b>Table No.</b>	<b>Title</b>	<b>Page</b>
2.1	Types of bearing damage, appearance, and possible causes	10
2.2	Result Tabulation	21
2.3	Types and location of defect	21
2.4	The fault description in the ball bearings	22
4.1	Wavelet coefficient value for each level decomposition at 287 rpm	47
4.2	Wavelet coefficient value for each level decomposition at 1466 rpm	48
4.3	Wavelet coefficient value for each level decomposition at 2664 rpm	50

## LIST OF FIGURES

Figure No.	Title	Page
1.1	Project's Flow Chart	5
1.2	Project's Gantt Chart	6
2.1	Rolling element bearing	9
2.2	The outer race defect of the tested bearing	12
2.3	Exploded view of bearing assembly	12
2.4	Vibration time waveform of (a) healthy bearing, and (b) defect bearing	16
2.5	Processes of signal within time and frequency domain	16
2.6	The STFT method	17
2.7	Comparison of known transformation methods	19
2.8	The actual bearing test rig	20
2.9	Sine wave with break of CWT method	23
2.10	Multi resolution time-frequency of form	24
2.11	Time-frequency analysis of CWT	24
2.12	Example of GUI simulations for fault detection system (broken bar)	25
3.1	Flow chart for CWT method analysis process	29
3.2	Design of the GUI layout.	31
3.3	Open the new sheet GUI (a) Type of GUI chosen, and (b) New GUI sheet appear.	32
3.4	(a) Selecting pushbutton, and (b)selecting axis	33
3.5	The complete layout of GUI	33
4.1	Vibration reading for the good condition of bearing on 287 rpm	35
4.2	Vibration reading for the good condition of bearing on 1466 rpm	36
4.3	Vibration reading for the good condition of bearing on 2664 rpm	37
4.4	Time domain for the good condition of bearing on 287 rpm and scalogram of wavelet analysis	38
4.5	Time domain for the good condition of bearing on 1466 rpm and scalogram of wavelet analysis	39
4.6	Time domain for the good condition of bearing on 2664 rpm and scalogram of wavelet analysis	39

4.7	Time domain for the contaminated defect on 287 rpm and scalogram of wavelet analysis	40
4.8	Time domain for the contaminated defect on 1466rpm and scalogram of wavelet analysis	40
4.9	Time domain for the contaminated defect on 2664 rpm and scalogram of wavelet analysis	41
4.10	Time domain for the inner race defect on 287 rpm and scalogram of wavelet analysis	41
4.11	Time domain for the inner race defect on 1466 rpm and scalogram of wavelet analysis	42
4.12	Time domain for the inner race defect on 2664 rpm and scalogram of wavelet analysis	42
4.13	Time domain for the outer race defect on 287 rpm and scalogram of wavelet analysis	43
4.14	Time domain for the outer race defect on 1466rpm and scalogram of wavelet analysis	43
4.15	Time domain for the outer race defect on 2664 rpm and scalogram of wavelet analysis	44
4.16	Time domain for the corroded defect on 287 rpm and scalogram of wavelet analysis	44
4.17	Time domain for the corroded defect on 1466 rpm and scalogram of wavelet analysis	45
4.18	Time domain for the corroded defect on 2664 rpm and scalogram of wavelet analysis	45
4.19	Wavelet coefficient vs. decomposition level for speed at 287 rpm	47
4.20	Wavelet coefficient vs. decomposition level for speed at 1466 rpm	49
4.21	Wavelet coefficient vs. level decomposition for speed at 2664 rpm	51
4.22	FFT result for corroded defect at 2664 rpm.	52
4.23	FFT graph for bearing at 287 rpm	53
4.24	FFT graph for bearing at 1466 rpm	54
4.25	FFT graph for bearing at 2664rpm	55
4.26	The result of GUI for defected bearing	56
4.27	The result of GUI for bearing in good condition	57



**LIST OF SYMBOL**

$\omega_s$	Shaft rotation frequency
$\alpha$	Contact angle
$\psi(t)$	Mother wavelet

**LIST OF ABBREVIATIONS**

ASiVR	Advance Structural Integrity & Vibration Research
CUI	Character User Interface
CWT	Continuous Wavelet Transform
DWT	Discrete Wavelet Transform
FFT	Fast Fourier Transform
GUI	Graphical User Interface
RPM	Revolutions per minute
STFT	Short Time Fourier Transform
WT	Wavelet Transform
WYSIWYG	What you see is what you get

## **CHAPTER 1**

### **INTRODUCTION**

#### **1.0 INTRODUCTION**

This chapter discusses the about the project background, problem statement, the objectives, scopes of project, project flow and project Gantt chart. Besides that, it also consists with the thesis overview for this project.

#### **1.1 PROJECT BACKGROUND**

Ball bearing failures can be caused by several factors, such as incorrect design or installation, acid corrosion, poor lubrication and plastic deformation (R. Rubini and U. Meneghetti 2000). Detecting or even preventing failures in complex machines usually benefits in terms of economy and security. However, defects can occur due to the great number of critical processes where bearings are employed. The precocious diagnosis of possible faults constitutes an important activity to prevent more serious damages.

Therefore, this type of fault must be detected as soon as possible to avoid fatal breakdowns of machines that may lead to loss of production. Bearing defects may be categorized as “distributed” or “local” (N. Tandon, A. Choudhury 1999). Distributed defects include surface roughness, waviness, misaligned races and off-size rolling elements. Localized defects include cracks, pits and spalls on the rolling surfaces. The

faulty bearing in the rotating parts or engineering components will excite the vibration signal with different behavior or structure. Therefore, the advance signal analysis is required to evaluate the vibration signatures from different type of bearing defect.

There are many condition monitoring methods used for detection and diagnosis of rolling element bearing defects such as wear debris analysis, temperature measurement, vibration measurement, and acoustic emission. Several techniques have been applied to measure the vibration and acoustic responses from defective bearings such as vibration measurements in time and frequency domains, the shock pulse method, sound pressure and sound intensity techniques and the acoustic emission method. Based on research mostly in last two decades, there are a lot work research on the detection and diagnosis of bearing defects by vibration and acoustic methods. Among these, vibration measurements are the most widely used (N. Tandon, A. Choudhury 1999).

## **1.2 PROBLEM STATEMENT**

The growing demand for high performance, efficiency, safety and reliability and increasing complexity of the technical processes has been of great interest in the development of fault detection methods (C. Angeli 2004). The early detection of faulty may help to avoid system breakdowns and product deterioration. Fault detection algorithms and their applications to a wide range of industrial processes has been the subject of intensive research over the past two decades. Existing methods for the fault detection have widely focused on the steady-state operations and are not directly applicable during the transitions. Recent results of studies show that more than 40% of induction motor failures are related to bearing (Tandon and Choudhury 1999). These data acquisition is a type of non-destructive which is does not required the user to dismantle the bearing from the machine in order to check its condition as it may be presented through online monitoring. In industries, high skill required from person in charge to know either the bearing is in good condition or not with or without dismantle the bearing from the machine.

### **1.3 OBJECTIVES**

The objectives of this project are:

- a) To develop software with signal processing tools to detect defect features in mechanical signal.
- b) To study a method to detect defect features in time-frequency domain for vibration signal
- c) To determine specific indicator in time and frequency domain to detect defect features

### **1.4 PROJECT SCOPES**

In order to reach the project's objectives, the following scopes are identified:

- a) Test four of bearing defect and they are inner race defect, outer race defect, contaminated defect, and corroded ball.
- b) Make a good condition bearing as the reference/datum.
- c) Graphical User Interface (GUI) analysis developed by using MATLAB
- d) Analysis method by using Continuous Wavelet Transform (CWT) method

### **1.5 PROJECT FLOW CHART**

In conducting a project, well arrangement of works and task is important to keep the momentum of this study. Figure 1.1 shows the flow chart for this project.

The process started with identify the problem statement especially problem face in industry, the objectives and scopes of this project. After that, the problem identification will follow the flow and continue with the finding the related journal or literature review about this title. It will help to gain the knowledge and also help to discuss about this project.

The next step will be continued in Final Year Project 2 (FYP2) which is the data will be analysed by using Continuous Wavelet Transform (CWT) method. The data had been acquired from previous study. At this step, the coding of the CWT method will generate in MATLAB software. After the result of the analysis had validation to detect the defect occurred in the bearing, it will be continued by developing the Graphical User Interface (GUI) in the MATLAB. Then, the result of the GUI will discuss and conclude the project.

Figure 1.2 shows the Gantt chart of this project which is for final year project 1 and 2. From the chart, there is some of the task is not follow the planning schedule. It is because there are some problem occurred when performing the task such as need to change the method because of validations the data with the result and also lack of knowledge of the software.

Basically, the project still moves on with the flow of the planning and had done within the time given.

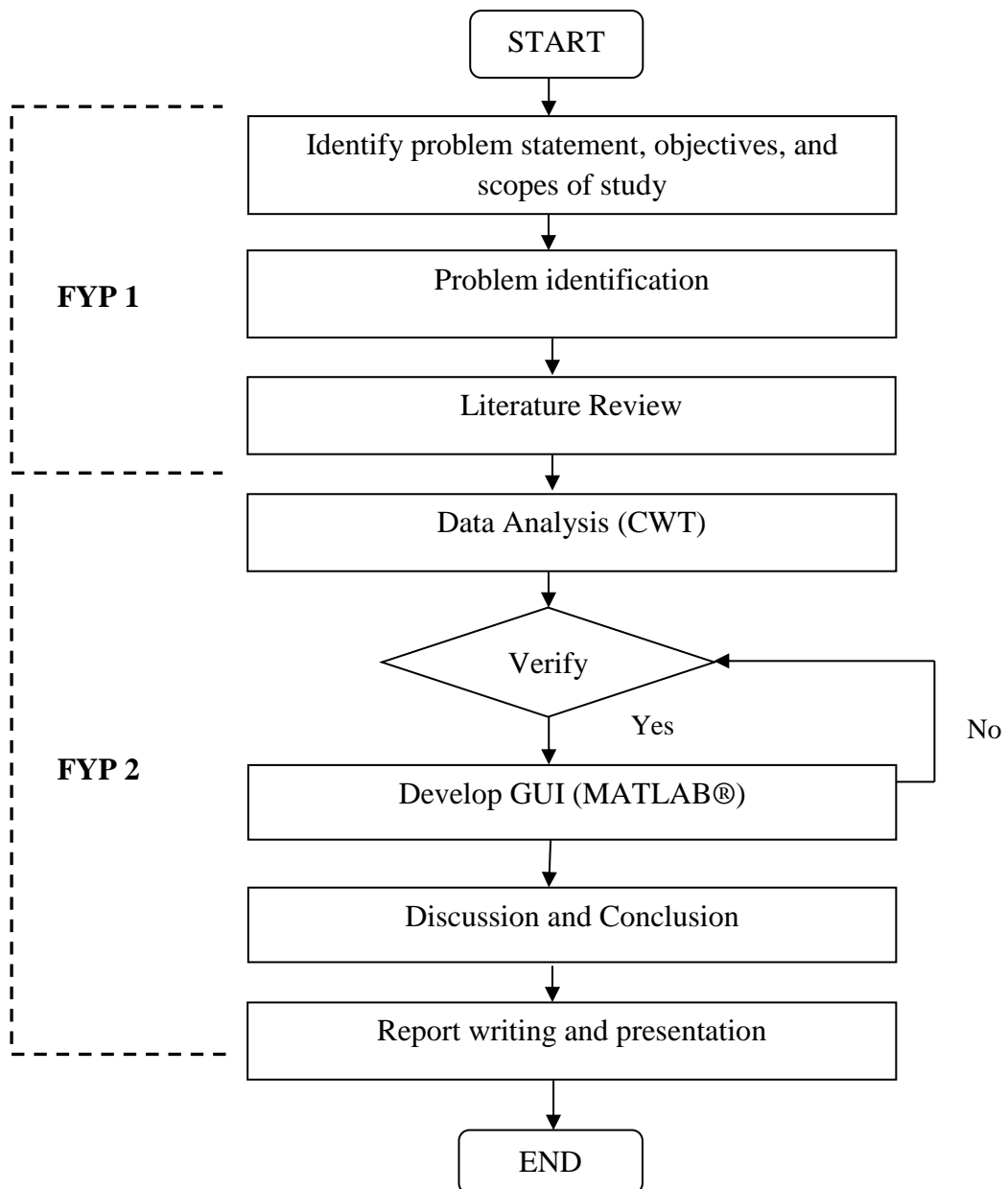


**Figure 1.1:** Project's Flow Chart

**FYP 1**

TASK		WEEK													
		1	2	3	4	5	6	7	8	9	10	11	12	13	14
Receive title and research	Plan	█	█												
	Actual	█	█	█											
Information research	Plan		█	█	█	█	█	█	█	█	█	█	█	█	█
	Actual			█	█	█	█	█	█	█	█	█	█	█	█
Research on CWT & GUI	Plan			█	█	█	█	█	█	█	█	█			
	Actual			█	█	█	█	█	█	█	█	█	█		
Installing and learn MATLAB Software	Plan				█	█	█	█	█						
	Actual				█	█	█	█	█	█	█	█			
Methodology	Plan				█	█	█	█	█	█	█	█	█		
	Actual					█	█	█	█	█	█	█	█	█	█
Data acquisition	Plan							█	█	█	█	█	█		
	Actual							█	█	█	█	█	█	█	█
Design layout GUI and framework CWT	Plan							█	█	█	█	█	█		
	Actual							█	█	█	█	█	█	█	█
Report preparation	Plan							█	█	█	█	█	█		
	Actual							█	█	█	█	█	█	█	█
Presentation preparation	Plan									█	█	█	█	█	█
	Actual									█	█	█	█	█	█

**FYP 1**

TASK		WEEK													
		1	2	3	4	5	6	7	8	9	10	11	12	13	14
Develop CWT coding	Plan	█	█	█	█										
	Actual	█	█	█	█	█									
Run CWT analysis	Plan				█	█	█								
	Actual				█	█	█	█	█	█					
Develop GUI layout and coding	Plan					█	█	█	█						
	Actual					█	█	█	█	█	█	█	█		
Run GUI	Plan							█	█	█	█				
	Actual							█	█	█	█	█	█		
Analysis data and discussion	Plan									█	█	█	█		
	Actual									█	█	█	█	█	█
Preparation draft thesis and slide presentation	Plan							█	█	█	█	█	█	█	
	Actual							█	█	█	█	█	█	█	█
Presentation FYP2	Plan													█	█
	Actual													█	█
Final report submission	Plan														█
	Actual														█

**Figure 1.1:** Project's Gantt chart



## **1.6 THESIS OVERVIEW**

Chapter 1 introduces the background of the study. It is continue with simple discussion about ball bearing defect, problem statement which related to the study, the objectives, and scope of the study, the flow chart and Gantt chart for this project and the overview of the thesis.

Chapter 2 presents the information of bearing, types of bearing defect, and signal processing. This chapter also will discuss about Continuous Wavelet Analysis (CWT) and Graphical User Interface (GUI). It also includes the bearing fault detection and condition monitoring method.

Chapter 3 includes the comprising methodology of this project. This chapter also will discuss about data acquisition, data processing analysis by using CWT method. This chapter will enclosed with the design layout of GUI and develop it by using MATLAB®.

Chapter 4 will present the result of the tabulation result or data and further discusses about the outcome of the analysis. It will show more detail about the development of GUI for bearing fault detection.

This study will enclosed by chapter 5 with the conclusion for this project and recommendation for future research.

## **CHAPTER 2**

### **LITERATURE REVIEW**

#### **2.0 INTRODUCTION**

This chapter discuss the literatures review related to bearing fault detection, Graphical User Interface (GUI) and Continuous Wavelet Transform (CWT). This title requires an amount of good understanding on the knowledge and executes a research is necessary to obtain the information are essentially valuable and suitable to assist in the construction of this project. In this chapter, it also explain discuss types of bearing and types of bearing defects, signal analysis, CWT, GUI, bearing fault detection and condition monitoring method.

#### **2.1 BEARING**

Bearing is a machine element that constrains relative motion between moving parts to only the desired motion. This mechanical device is typically in between linear and rotational movement (Richard H. 1997). There are many types of bearing often used in machinery field and each of them had their own purpose itself. Inventions of bearings such as roller bearing, hydrodynamics, hydrostatics and magnetic bearing, fluid bearing, and also flexure bearing made it possible to operate a shaft induced in load and high

speed while jewel bearing and plain bearing just required in load and low speed (Purtell, John 2000).

Roller bearing as shown in Figure 2.1 is a bearing which carries a load by placing round elements between two bearing rings. It is very easy to use in various equipment by its rolling facility. It is widely used because of the advantages of a good trade-off between cost, size, weight, carrying capacity, durability, accuracy, friction, and etc. (Harris, Tedric A. 2000).



**Figure 2.1:** Roller bearing

**Source:** FAG 2006

### **2.1.1 Types of Bearing Defects**

Bearings are among the most important components in the vast majority of machines and exacting demands are made upon their carrying capacity and reliability. Unfortunately it sometimes happens that a bearing does not attain its calculated rating life. Each of the different causes of bearing failure produces its own characteristic damage known as primary and secondary damage. Primary damage consists of wear indentations, smearing, surface distress, corrosion, and electric current damage. Secondary damage includes flaking and cracks.

Table 2.1 shows the different types of bearing damage, its appearance, and causes of this damage. Each type of defect has own characteristic and also appearance. Some of the defect has come with the same causes but the differentiation between them is the appearance defect itself.

**Table 2.1:** Types of bearing damage, appearance, and possible causes.

<b>Types of damage</b>	<b>Appearance</b>	<b>Causes</b>
Wear	<ul style="list-style-type: none"> <li>• Small indentations around the raceway and rolling element</li> <li>• Grease discolored green</li> <li>• Wear on inner/outer rings</li> </ul>	<ul style="list-style-type: none"> <li>• Lack of cleanliness during mounting</li> <li>• Ineffective seals</li> <li>• Sliding abrasion, bearing of insufficient hardness, contamination by foreign matter shortage of lubricant, improper lubrication</li> </ul>
Indentations	<ul style="list-style-type: none"> <li>• Indentations in the raceways of both rings with spacing equal to the distance between the rolling elements</li> <li>• Small indentations distributed around the raceways of both rings and in the rolling elements.</li> </ul>	<ul style="list-style-type: none"> <li>• Mounting pressure applied to the wrong ring</li> <li>• Excessively hard drive-up on tapered seating</li> <li>• Ingress of foreign particles into the bearing.</li> </ul>
Cracks	<ul style="list-style-type: none"> <li>• Bearing ring has cracked right through and has lost its grip on the shaft.</li> </ul>	<ul style="list-style-type: none"> <li>• Excessive drive-up on a tapered seating or sleeve.</li> </ul>
Surface Distress	<ul style="list-style-type: none"> <li>• Small, shallow craters with crystalline fracture surfaces</li> </ul>	<ul style="list-style-type: none"> <li>• Inadequate or improper lubrication.</li> </ul>
Flaking	<ul style="list-style-type: none"> <li>• Heavily marked path pattern in raceways of both rings.</li> <li>• Usually in the most heavily loaded zone.</li> <li>• Heavily marked path pattern at two diametrically opposed sections of either bearing ring.</li> </ul>	<ul style="list-style-type: none"> <li>• Preloading on account of fits being too tight.</li> <li>• Excessive drive-up on a tapered seating</li> <li>• Oval shaft or oval housing seating.</li> </ul>
Corrosion	<ul style="list-style-type: none"> <li>• Greyish black streaks across the raceways</li> <li>• Raceway path pattern heavily marked at corresponding positions.</li> </ul>	<ul style="list-style-type: none"> <li>• Presence of water, moisture</li> <li>• Shaft or housing seating with errors of form.</li> </ul>

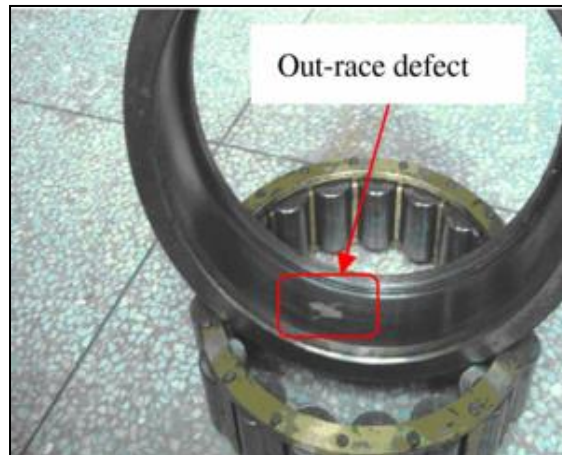
**Table 2.1:** Continued

<b>Types of damage</b>	<b>Appearance</b>	<b>Causes</b>
Smearing	<ul style="list-style-type: none"> <li>• Scored and discolored roller ends and flange faces.</li> <li>• Scored and discolored areas at the start of the load zone in raceways and on the surface of the rollers.</li> <li>• Scored and discolored ring bore or outside surface or faces.</li> <li>• Scored and discolored ring bore or outside surface or faces.</li> </ul>	<ul style="list-style-type: none"> <li>• Sliding under heavy axial loading and with inadequate lubrication.</li> <li>• Roller acceleration on entry into the loaded zone.</li> <li>• Ring rotation relative to shaft or housing.</li> <li>• Ring rotation relative to shaft or housing.</li> </ul>
Electric Current	<ul style="list-style-type: none"> <li>• Dark brown/greyish black fluting (corrugation) or craters in raceways and rollers.</li> <li>• Localized burns in raceways and on rolling elements</li> </ul>	<ul style="list-style-type: none"> <li>• Passage of electric current through rotating bearing.</li> <li>• Passage of electric current through non-rotating bearing.</li> </ul>

**Source:** SKF Handbook 1994

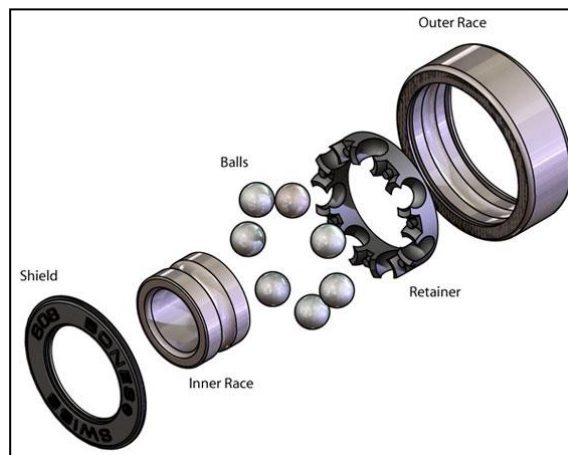
There are four common categories of bearing fault which are outer race, inner race, ball and cages. Bearing defect usually occur on three area of the bearing which are the outer race, inner race and the ball bearing itself (Martin and Honarvar 1994). Usually this failure occurred according by either overloading, over speeding or also starving of lubrication.

Figure 2.2 show the outer race defect of the tested bearing. The outer race is the retainer or holder for all bearing assembly whereas the outer most surfaces will be contact with the bearing holder mechanism in a shaft assembly or any machinery assembly. Figure 2.3 shows the exploded view of bearing assembly



**Figure 2.2:** The outer race defect of the tested bearing

**Source:** Measurement and Technology 2012



**Figure 2.3:** Exploded view of bearing assembly

**Source:** Bones Baring 2011

The other part retainer of a ball bearing assembly also includes the inner race but it only for the inner part. The inner also is the most surfaces in direct contact with a shaft in a pump or machinery assembly.

The ball is one of the most important parts in a ball bearing. It acts as less friction characteristic in a high speed rotation usage contributed most form. On these two areas of outer and inner race, there is also the defect that usually found on this area such as point defect, line defect and rough defect.

## **2.2 SIGNAL ANALYSIS**

Signal processing is an area of engineering, electrical and applied mathematics that deals with operations on or analysis of signals, measurements of time-varying or spatially varying physical quantities. Signals of interest include sound, images, and sensor data, like biological data such as electrocardiograms, control system signals, telecommunication transmission signals, and etc. (Schafer, Ronald W. 1975).

### **2.2.1 Frequency Domain Analysis**

Frequency domain is a method used to analyze data. This refers to analyzing a mathematical function or a signal with respect to the frequency. Frequency domain analysis is widely used in fields such as control systems engineering, electronics and statistics. Frequency domain analysis is mostly used to signals or functions that are periodic over time

The advent of modern Fast Fourier Transform (FFT) analyzers to obtain narrowband spectra became easier and more efficient. Both low and high frequency ranges of the vibration signal or spectrum are of interest in assessing the condition of the bearing (Tandon and Choudhury 1999).

Each bearing elements has their own characteristics rotational frequency. There's an increase in vibration energy at the element's rotational frequency whenever there is a defect on a particular bearing. These characteristic defect frequencies can be calculated from kinematic considerations. For a bearing with a stationary outer race, these frequencies are given by the following expressions:

Cage frequency  $\omega_c$ , proposed by Mathew and Alfredson (1984) as in Eq. 2.1:

$$\omega_c = \frac{\omega_s}{2} \left( 1 - \frac{d}{D} \cos \alpha \right) \quad (2.1)$$

Ball spinning frequency  $\omega_b$ , as in Eq. 2.2 proposed by McFadden and Smith (1984a):

$$\omega_b = \frac{D\omega_s}{2d} \left( 1 - \frac{d^2}{D^2} \cos^2 \alpha \right) \quad (2.2)$$

Outer race defect frequency  $\omega_{OD}$ , proposed by Kim (1984a) as in Eq. 2.3:

$$\omega_{OD} = Z\omega_c = \frac{Z\omega_s}{2d} \left( 1 + \frac{d}{D} \cos \alpha \right) \quad (2.3)$$

Inner race defect frequency  $\omega_{ID}$ , as in Eq. 2.4 proposed by Kim (1984b):

$$\omega_{ID} = Z(\omega_s - \omega_c) = \frac{Z\omega_s}{2} \left( 1 + \frac{d}{D} \cos \alpha \right) \quad (2.4)$$

and

Rolling element defect frequency  $\omega_{rc}$ , proposed by Sunnersjo (1978) as in Eq. 2.5:

$$\omega_{rc} = 2\omega_b = \omega_s \frac{D}{d} \left( 1 + \frac{d^2}{D^2} \cos^2 \alpha \right) \quad (2.5)$$

where,

$\omega_s$  is the shaft rotation frequency in rad/s

$d$  is the diameter of the rolling element

$D$  is the pitch diameter

$Z$  is the number of rolling element, and

$\alpha$  is the contact angle.



As the impact vibration generated by a bearing fault has relatively low energy, it is often overwhelmed by noise with higher energy and vibration generated from other macro structural components. Therefore, it is difficult to identify the bearing fault in the spectra using the conventional FFT method, and hence advanced signal processing techniques are needed.

### **2.2.2 Time Domain Analysis**

Time domain analysis analyzes the data over a time period. Functions such as electronic signals, market behaviours, and biological systems are some of the functions that been analyzed using time domain analysis. In a time domain analysis, the variable is always measured against time.

When faulty occur in a bearing, abnormal behaviour can be seen from the vibration signals. The easiest way is visually inspect portions of time domain waveform. Figure 2.4 shows the vibration signal taken from a bearing in good and defect condition. From the waveform, the signal of healthy bearing shows more stable or other word is its amplitude same alike with others but in defective bearing signal, there are very different amplitude to each other and also there is some noise of high peak compare to the healthy one.

Signals can be transformed between the time and the frequency domain through various transforms. The signals can be processed within these domains and each process in one domain has a corollary in the other, as shown in figure 2.5:

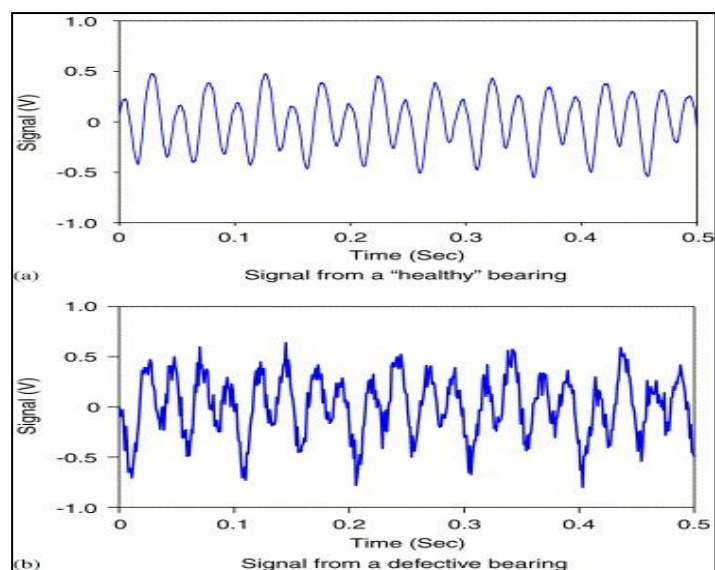


**Figure 2.4:** Vibration time waveform of (a) healthy bearing, and (b) defect bearing.

**Source:** Robotics and Computer-Integrated Manufacturing 2005

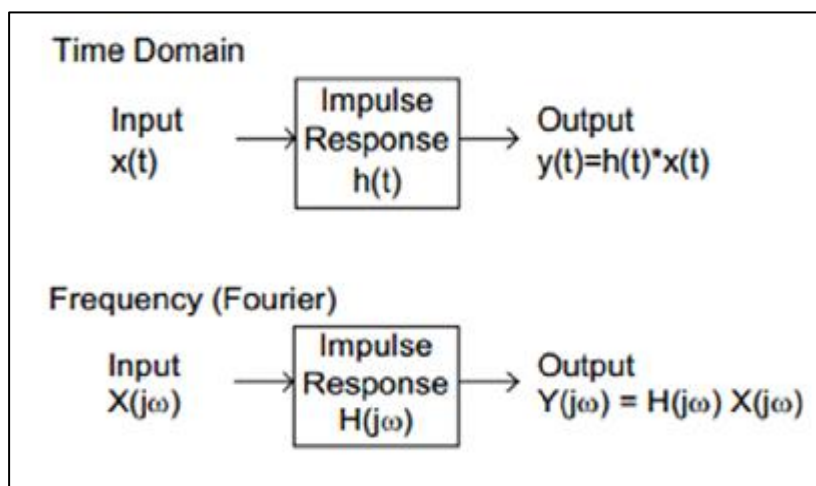


**Figure 2.5:** Processes of signal within time and frequency domain

**Source:** MITx 2011

There are several methods used to analyze data on a time-frequency domain analysis such as Short Time Fourier Analysis (STFT), and Discrete Wavelet Transform (DWT).

The Short Time Fourier Transform (STFT) represents a sort of compromise between the time- and frequency-based views of a signal. It provides some information about both when and at what frequencies a signal event occurs. It functioned as to determine the sinusoidal frequency and phase content of local sections of a signal as it changes over time and only can obtain this information with limited precision, and that precision is determined by the size of the window. Figure 2.6 shows the STFT method.

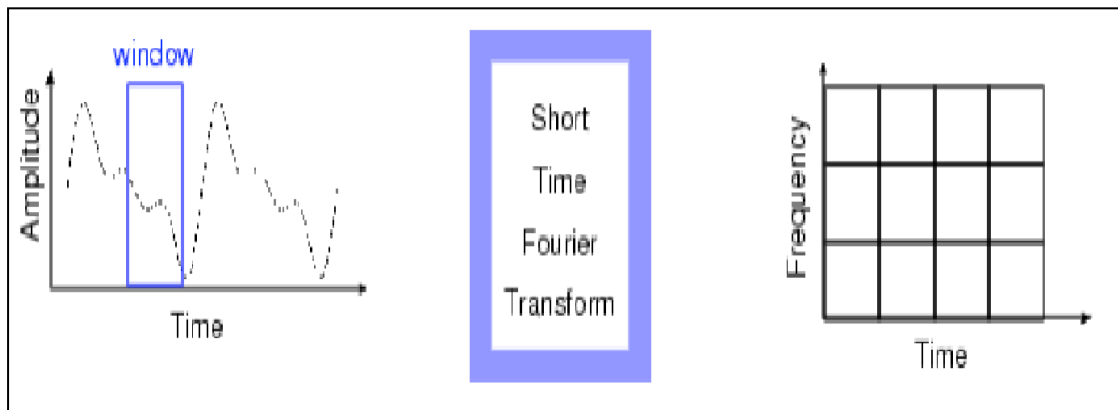


**Figure 2.6:** The STFT method

**Source:** The MathWorks 1984-2007

The transform of a signal is just another form of representing the signal. It does not change the information content present in the signal. The Wavelet Transform (WT) provides a time-frequency representation of the signal. This property makes wavelets an ideal tool for analyzing signal of a transient or non-stationary nature (Prabakhar, 2002). It was developed to overcome the short coming of the STFT, which can also be used to analyze non-stationary signals. While STFT gives a constant resolution at all frequencies, the Wavelet Transform uses multi-resolution technique by which different frequencies are analyzed with different resolutions.

The Continuous Wavelet Transform (CWT) of  $f(t)$  is a time scale method that may be identified as the sum over all time of the signal multiplied by scale, shifted versions of the wavelet function  $\psi(t)$ . This formula was proposed by McFadden and Smith (1984b) as shown below in Eq. 2.6:

$$CWT(a,b) = \frac{1}{\sqrt{|a|}} \int_{-\infty}^{\infty} f(t) \Psi^* \left( \frac{t-b}{a} \right) dt \quad (2.6)$$

where  $\psi(t)$  denotes the mother wavelet the basis function. The translation parameter  $a$  mean relates to the location of the wavelet function as it is shifted through the signal. The scale parameter  $b$  is defined as  $|1/\text{frequency}|$  and corresponds to frequency information.

The DWT is derived from the discretization of CWT  $(a,b)$  and the most common discretization is dyadic, also given by McFadden and Smith in 1985 as in Eq. 2.7,

$$DWT(j,k) = \frac{1}{\sqrt{2^j}} \int_{-\infty}^{\infty} f(t) \Psi^* \left( t - \frac{2^j k}{2^j} \right) dt \quad (2.7)$$

where  $a$  and  $b$  are replaced by  $2^j$  and  $2^j k$ . An effective way to apply this method using filters was developed by Mallat in 1989. The  $f(t)$  passes through two complementary filters and emerges as low and high frequency signals. The decomposition may be iterated with successive approximations begin decomposed in turn, so that signals may be broken down into lower resolution components.

Figure 2.7 shows the comparison of four transformation methods. Time domain analysis has a better time resolution while frequency (Fourier Transform) has a better frequency resolution. While STFT is equal on both where it has fixed resolution, DWT on the other hand provides time scale information of a signal, enabling the extraction of features that varies in time.

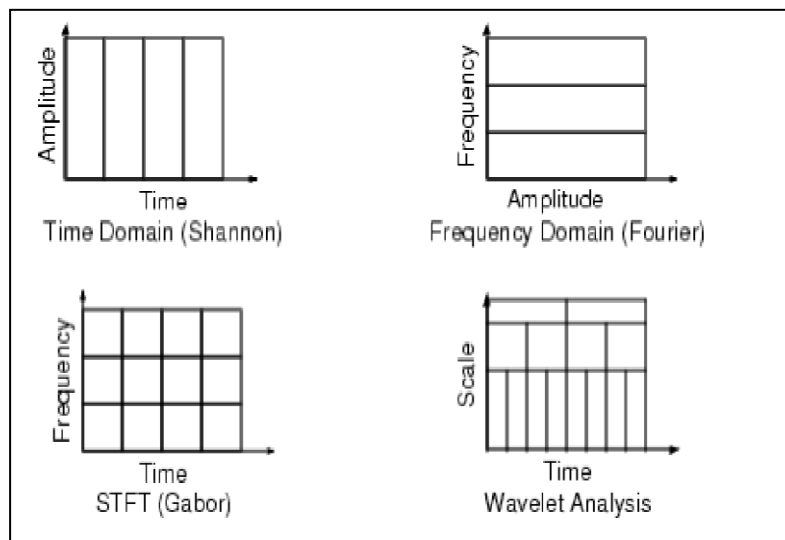


**Figure 2.7:** Comparison of known transformation methods.

**Source:** The MathWorks 1984-2007

### 2.3 BEARING FAULT DETECTION

Vibration monitoring is the most widely used and cost effective monitoring technique to detect, locate and distinguish faults in ball bearings (Manish Yadav 2011). When a localized fault in a bearing surface strikes another surface, impact vibrations are generated. Condition monitoring is performed by analyzing the changes in the vibration signature due to the presence of these impulses. Faulty diagnosis helps to identify the location of the fault so that corrective action can be taken and maintenance can be planned accordingly.

Detecting rolling element bearing faults is the highest priority for most vibration analysts. Detecting the fault at the earliest opportunity should be the priority, however in reality most analysts do not detect the fault in the first or even the second stage of failure.

Bearing faults can take place due to fatigue even under normal balanced operation with good shaft alignment and can also be caused by improper lubrication, installation errors and contamination. One of the results of bearings failures are increased level of vibration and noise.

The test rig for bearing fault detection experiment was design to investigate failure and vibration characteristic of ball bearing. It was built to simulate real world pump mechanism where ball bearing plays a major role in rotational machinery. The shaft was driven by a variable speed with a frequency converter in order to control the speed of motor. The shaft will connected to motor for minimize shaft alignment error by using spring coupling. The angular speed is set to 287 rpm, 1466 rpm, and 2664 rpm. Sensors were placed on horizontal directions to collect data because this test based on horizontal bearing type. For each speed and type of bearing, fifty data will be collected due to the motor range of minimum to maximum operation. Finally, the vibration data is acquired using accelerometer. Figure 2.8 below shows the actual bearing test rig of detecting fault bearing and Table 2.2 shows the summary of this experiment while Table 2.3 shows the type and location of defect for six bearing that were tested for this experiment.



**Figure 2.8:** The actual bearing test rig

**Source:** Bearing Fault Detection 2012

**Table 2.2:** Result Tabulation

<b>Types of Defect</b>	<b>Location of Defect</b>
Outer Race Defect	One scratch mark on the outer race
Inner Race Defect	One scratch mark on the inner race
Point Defect	Single point mark on the inner race
Contaminated Defect	Lubrications was contaminated with tiny chips
Corroded Defect	Ball bearing were left to open air and water

**Table 2.3:** Types and location of defect

<b>Experiment</b>	<b>Speed (rpm)</b>	<b>Bearing Type</b>
1-5	287 / 1466 / 2664	Healthy Bearing
6-10	287 / 1466 / 2664	Outer Race Defect
11-15	287 / 1466 / 2664	Inner Race Defect
16-20	287 / 1466 / 2664	Point Defect
21-25	287 / 1466 / 2664	Contaminated Defect
26-30	287 / 1466 / 2664	Corroded Defect

## 2.4 CONDITION MONITORING

There are various methods used throughout the whole world for condition monitoring. There are some argument among researcher on which methods gives the best required and most precise and accurate result. The signals of rolling bearings faults are usually transient and modulated by high frequency carrier signal (Khalid, 2007). The damaged bearing used including outer race, inner race, and ball defects and also consists a good/healthy bearing as a reference. Table 2.4 shows the fault description in the ball bearings

**Table 2.4:** The fault description in the ball bearings

<b>Location of Defect</b>	<b>Types of Defect</b>
Healthy bearing	No scratch mark
Inner race (on the track)	One scratch mark
Outer race (on the track)	One scratch mark
Outer race ( 180 apart on the track)	Two scratch mark
Inner race (on the track) and outer race (on the track)	One scratch mark on each race

**Source:** Prabhakar 2002

## 2.5 CONTINUOUS WAVELET TRANSFORM

The Wavelet Series is just a sampled version of CWT and its computation may consume significant amount of time and resources, depending on the resolution required. In CWT, the signals are analyzed using a set of basic functions which relate to each other by simple scaling and translation.

The Continuous Wavelet Transform allows us to see the correlation of all the different lengths wavelets to the signal itself in the time domain. Use the CWT command in MATLAB® to obtain the transform. What is interesting about this transform, unlike the Fourier transform, is that it allows one to see breaks within the original signal and the exact position of those breaks as seen in the following Figure 2.9.

The STFT provide a means of (joint) time-frequency analysis with the property that spectral or temporal widths (or resolutions) were the same for all basis elements.



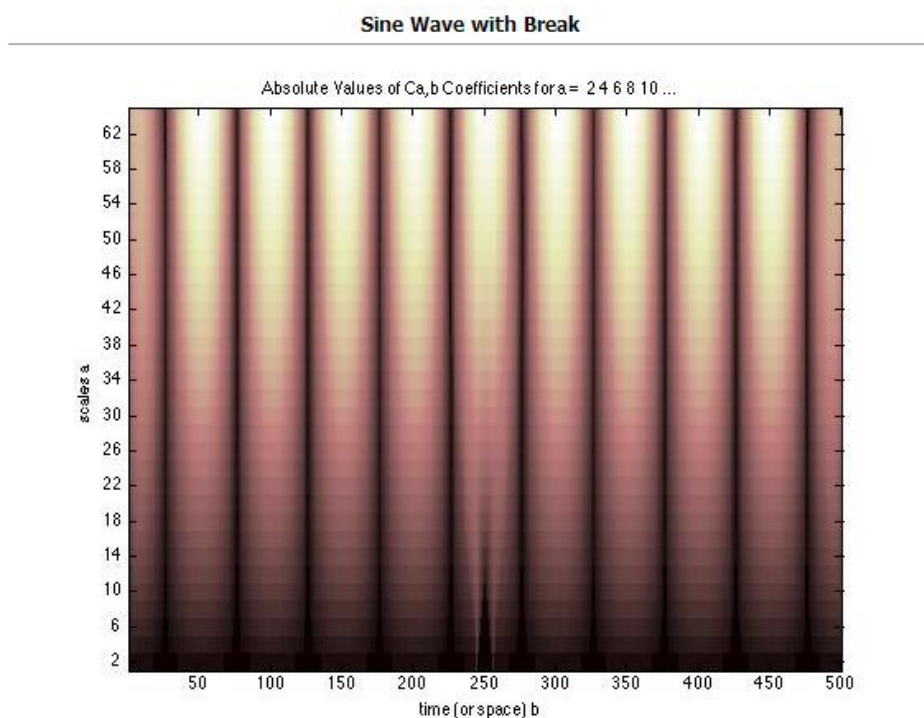


**Figure 2.9:** Sine wave with break of CWT method

**Source:** Aniruddha Sen 2011

To see the implication of uniform resolution, two signals composed of sinusoids with frequency 1 Hz and 1.001 Hz, respectively been considered. It may be difficult to distinguish between these two signals in the presence of background noise unless many cycles are observed, implying the need. Now consider two signals with pure frequencies of 1000 Hz and 1001 Hz-again, a 0.1% difference. Here it should be possible to distinguish the two signals in an interval of much less than one second. In other words, good frequency resolution requires longer observation times as frequency decreases. Thus, it might be more convenient to construct a basis whose elements have larger temporal width at low frequencies. The previous example motivates a multi-resolution time-frequency tiling of the form as shown in Figure 2.10.

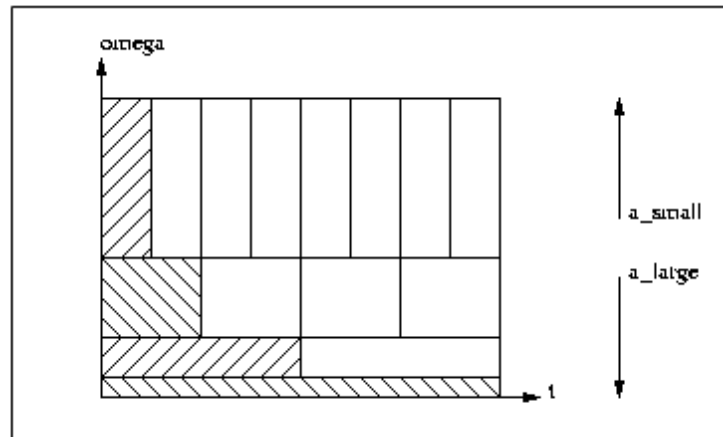


**Figure 2.10:** Multi resolution time-frequency of form

**Source:** Phil Schniter 2009.

The CWT accomplishes the above multi-resolution tiling by time-scaling and time-shifting a prototype function  $\psi(t)$ , often called the mother wavelet. In basis terms, the CWT says that a waveform can be decomposed into a collection of shifted and stretched versions of the mother wavelet  $\psi(t)$ . As such, it is usually said that wavelets perform a "time-scale" analysis rather than a time-frequency analysis as shown in Figure 2.11.

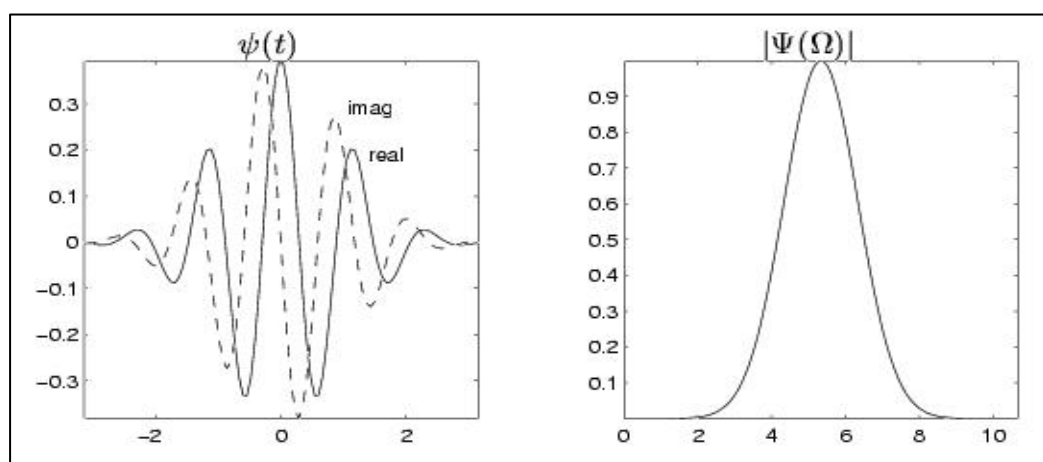


**Figure 2.11:** Time-frequency analysis of CWT

**Source:** Phil Schniter 2009.

## 2.6 GRAPHICAL USER INTERFACE

A graphical user interface (GUI) is a graphical display in one or more windows containing controls, called components that enable a user to perform interactive tasks. The user of the GUI does not have to create a script or type commands at the command line to accomplish the tasks. Unlike coding programs to accomplish tasks, the user of a GUI need not understand the details of how the tasks are performed. GUIs created using MATLAB tools can also perform any type of computation, read and write data files, communicate with other GUIs, and display data as tables or as plots.

Graphical User Interface (GUI) is a interact with computer using pictures and symbols, rather than having to memorize many complicated commands and type them precisely, as with a command-line interface. The actions are usually performed through direct manipulation of the graphical elements (Ziff Davis 2008). The term GUI is restricted to the scope of two-dimensional display screens with display resolutions able to describe generic information. Figure 2.12 shows the example of GUI simulations for fault detection system (broken bar).

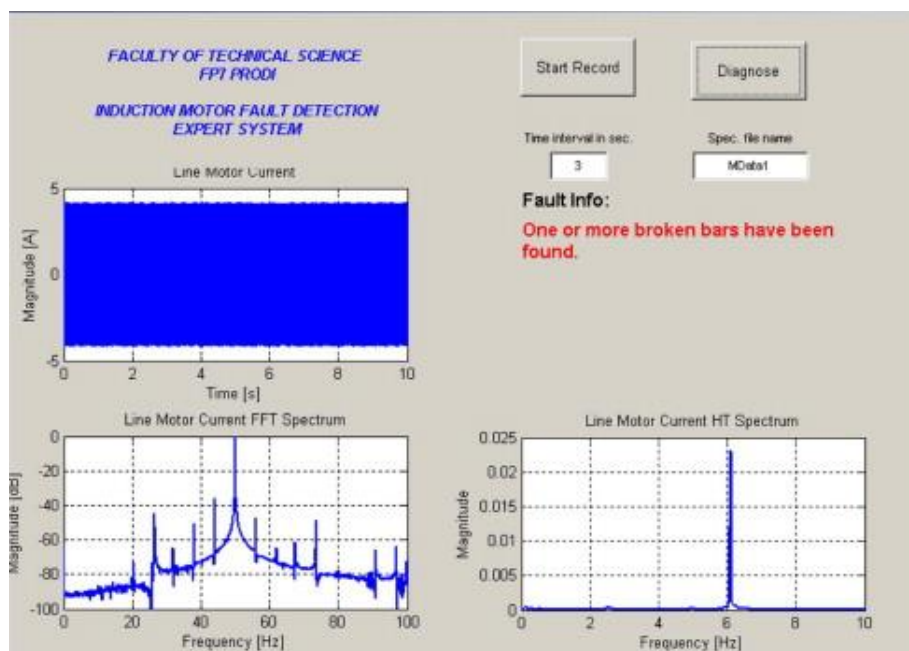


**Figure 2.12:** Example of GUI simulations for fault detection system (broken bar)

**Source:** Dragan Matic 2012

The main advantage of a Graphical User Interface is that it makes use of the WYSIWYG (What you see is what you get) method of representation of logical objects (like files, folders etc.). This is a much user- friendly platform than the CUI (Character User Interface) which requires the user to memorize a lot of commands, syntaxes and parameters in order to be able to work on the CUI.

## **CHAPTER 3**

### **METHODOLOGY**

#### **3.0 INTRODUCTION**

It is furthered with countless literature review throughout the whole project. Data used are obtained from previous study, and was analyzed by CWT method using MATLAB®. It will continue by designing layout of GUI, and the data was further processed by using MATLAB® to develop software with signal processing tools to detect defect features in vibration signal.

#### **3.1 DATA PROCESSING**

For this project, MATLAB® software was used to develop an algorithm to analyse the failure data. Algorithm developed includes analysis in frequency domain and also time-frequency domain.

##### **3.1.1 Continuous Wavelet Transform**

The basic objective of the wavelet transform is to achieve a complete time-scale representation of localised and transient phenomena occurring at different time scales.

Time-scale discrimination is achieved in a more satisfactory way than with time–frequency decompositions such as windowed Fourier or Gabor methods (Gabor 1946).

Figure 3.1 shows the flow chart for CWT method processing by using MATLAB® command. Input data which is the raw data will be loaded. The MATLAB® code needed to load the desired data is:

```
A = xlsread('good10.xlsx');
data=A(122881:126976,2);
```

where good10.xlsx is the file name while A is the length of the data that will be used in CWT analysis.

In engineering applications, the square of the modulus of the CWT is often called as scalogram, which has been widely used for fault diagnostics. When the complex wavelet is used, the wavelet transform can provide the amplitude and phase information of the signals simultaneously. The phase spectrum can be calculated easily from the wavelet transform.

It is well known that the CWT brings a lot of redundancy into the representation of the signal (a one-dimensional signal is mapped to a two-dimensional plane). As a result, there are several possibilities to reconstruct the signal  $x(t)$  from its CWT coefficients. The MATLAB® code needed to generate coefficient by using wavelet analysis is:

```
[f,coefs,t]=WaveletAnalysis(data,4097,20000,4096,'db4');
function[f,coefs,t]=WaveletAnalysis(Signal,ScaleLength,fs,bs,
wavename)
t=[0:bs-1].*(1/fs);
wcf=centfrq(wavename);
```

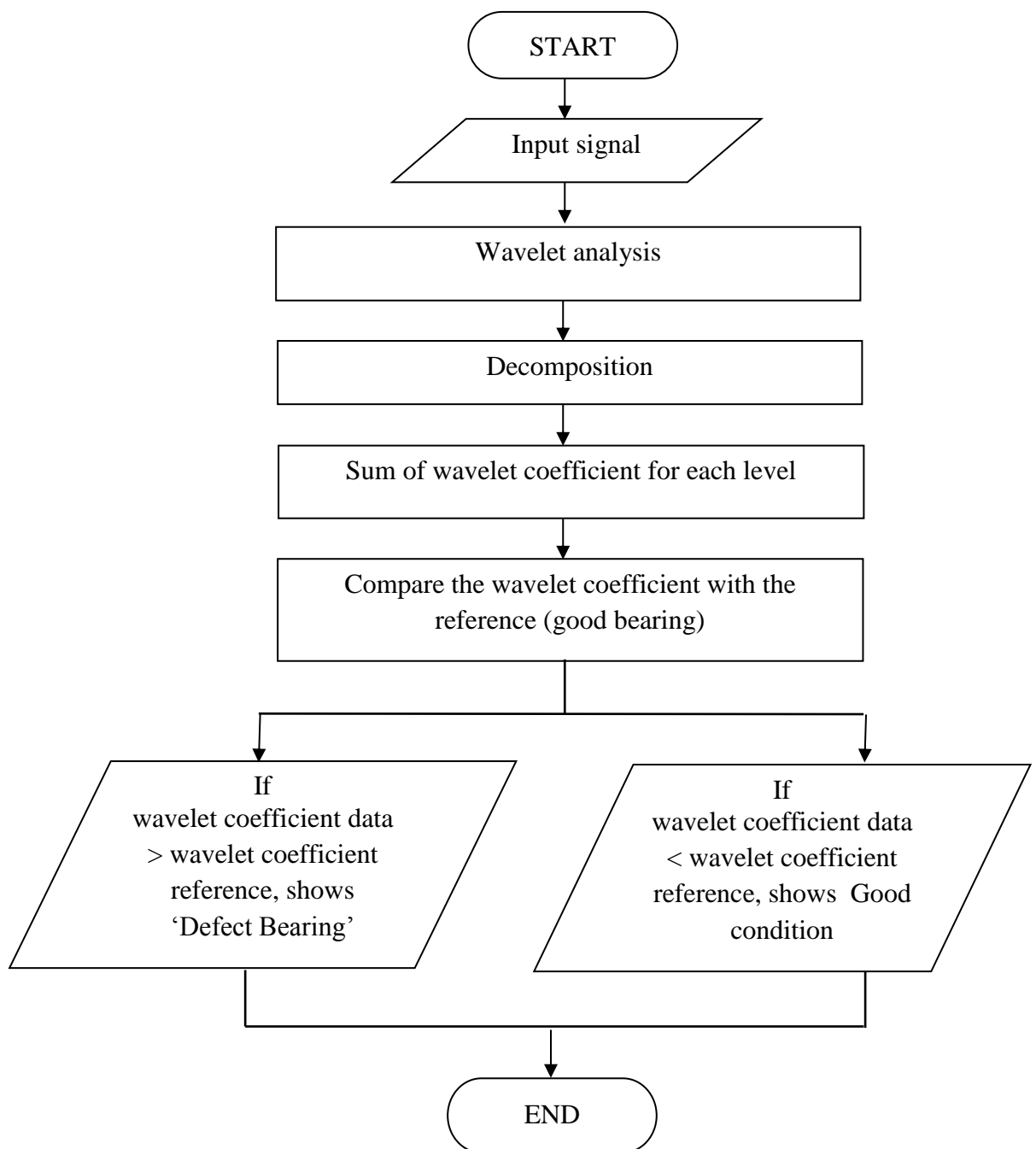


**Figure 3.1:** Flow chart for CWT method analysis process.

As a consequence, the main property of the wavelet transform is to make possible a time-scale discrepancy of processes. This allows, for example, distinguishing between two signals, which have very similar Fourier spectra. The CWT coefficients

indicate continuous and subtle information about the traffic flow signals. The CWT multiresolution coefficients map provides a powerful tool for identifying self-similarity and fractal patterns in the traffic flow. The MATLAB® code needed to generate wavelet coefficient for each level is:

```
% Calculate coefficient each level
D=abs (sum (coefs (1:4096, :))) ;
D1=abs (sum (coefs (1:2047, :))) ;
D2=abs (sum (coefs (1:1023, :))) ;
D3=abs (sum (coefs (1:511, :))) ;
D4=abs (sum (coefs (1:255, :))) ;
D5=abs (sum (coefs (1:127, :))) ;
D6=abs (sum (coefs (1:63, :))) ;
D7=abs (sum (coefs (1:31, :))) ;
D8=abs (sum (coefs (1:15, :))) ;
% Calculate sum wavelet coefficient each level
wc1=abs (sum (D1)) ;
wc2=abs (sum (D2)) ;
wc3=abs (sum (D3)) ;
wc4=abs (sum (D4)) ;
wc5=abs (sum (D5)) ;
wc6=abs (sum (D6)) ;
wc7=abs (sum (D7)) ;
wc8=abs (sum (D8)) ;
```

### **3.2 DEVELOPMENT OF GRAPHICAL USER INTERFACE**

A graphical user interface (GUI) is a graphical display in one or more windows containing controls, called components that enable a user to perform interactive tasks. Developing software with signal processing tools as function as detecting the defect features in mechanical signal will be presenting in GUI view.



The development will start off with design the layout of GUI to perform the task. Figure 3.2 shows the design of the GUI layout that will be the processing tool for detecting defects occurs in bearing.

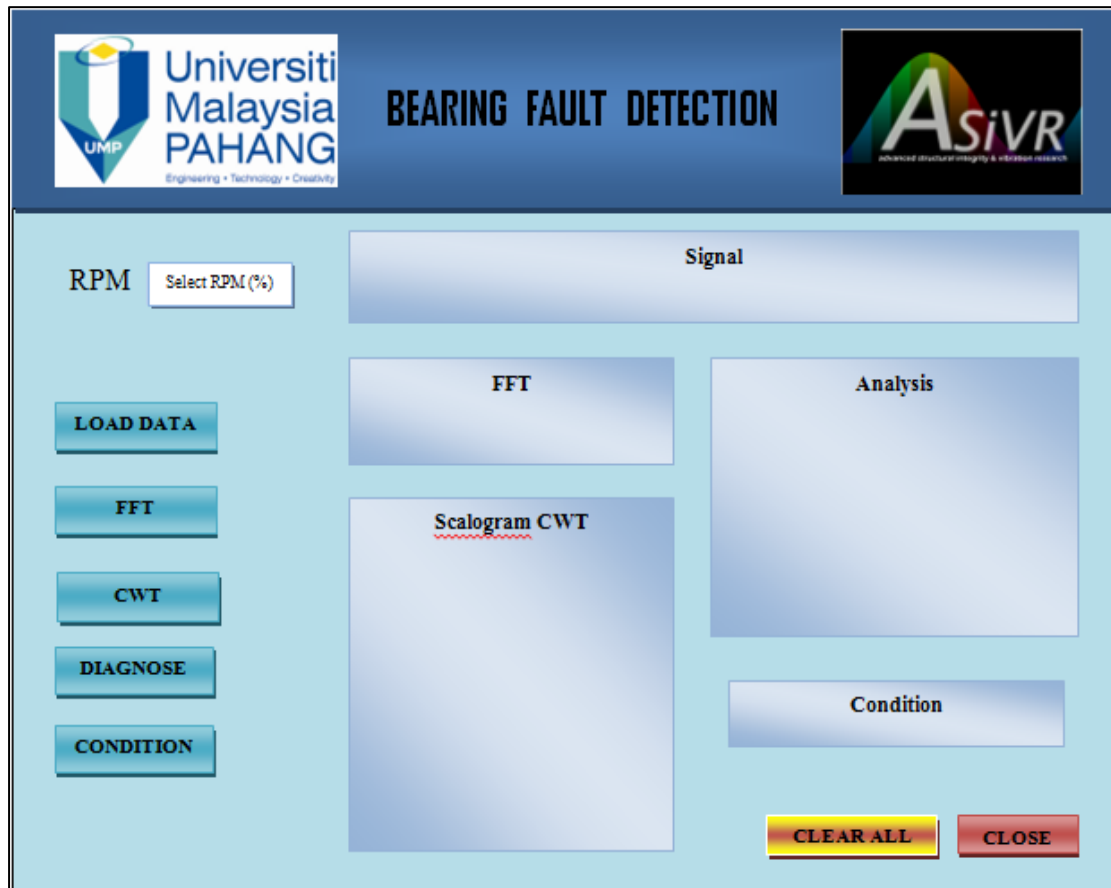
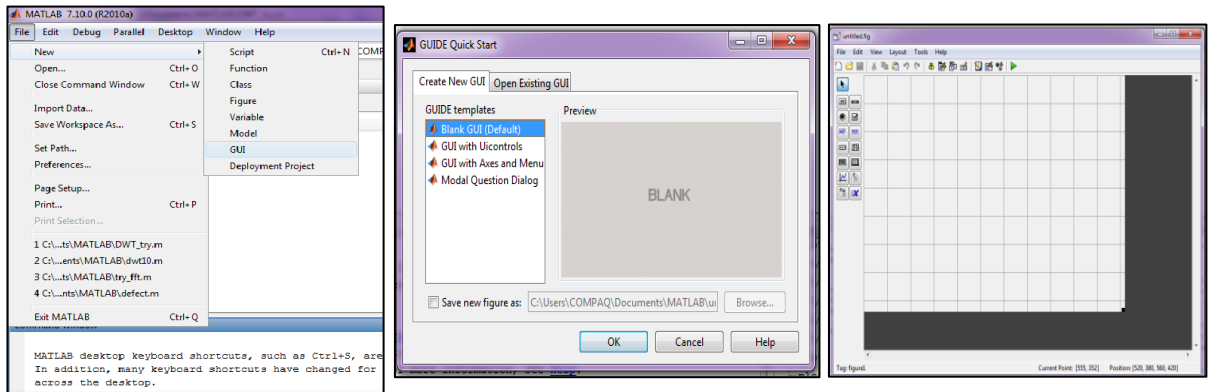


**Figure 3.2:** Design of the GUI layout.

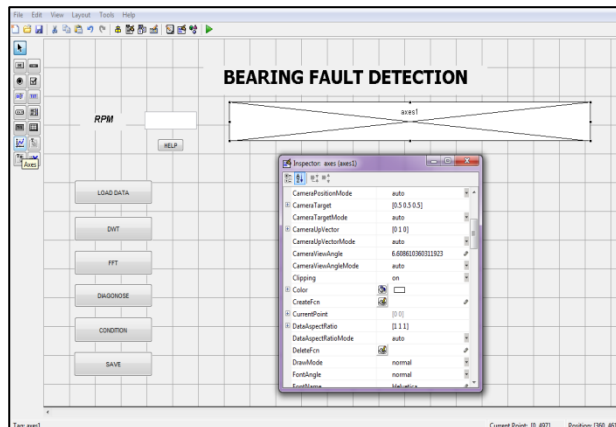
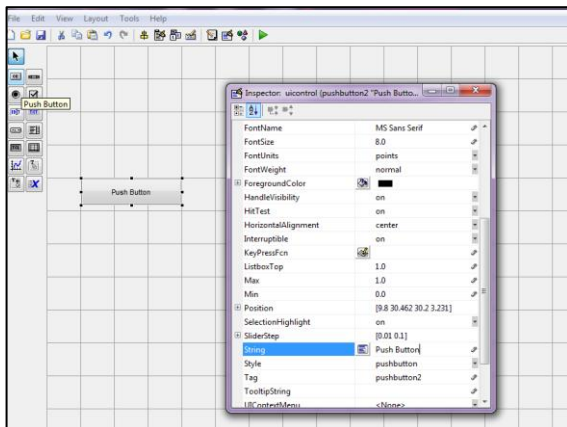
After the design was relevant with the scope and approached by supervisor, the step was further by develop it on the MATLAB® software. The processes start with the opening the MATLAB® program and wait for it to finish loading. Then, click on 'File' on MATLAB® in the launch pad and click 'New' for GUI as shown in Figure 3.3 (a). After that, choose for the 'Blank GUI (Default)' for starting design the layout by clicking OK as shown in Figure 3.3 (b). The new blank GUI sheet will appear as shown in Figure 3.3 (c).



(a) (b) (c)

**Figure 3.3:** (a) Open the new sheet GUI, (b) choose the type of GUI, and (c) new GUI sheet appear.

Next is to draw the layout by clicking a pushbutton on the left hand side of the window. This will allow you to drag and drop pushbutton. Double click on the pushbutton you just created. A property manager will pop up as shown in Figure 3.4 (a). Find the button on the left labelled "txt" and change the string name at the property manager as title of the layout which is 'Bearing Fault Detection'. Figure 3.4 (b) shown the ways to pop up the axis/chart view by clicking button 'axes' on the left side and also change the string name at the property manager for easier find and setup for each chart appear. Figure 3.5 shows the complete designing the layout of GUI before attached the command for each button.



(a)

(b)

Figure 3.4: (a) Selecting pushbutton, and (b) selecting axis

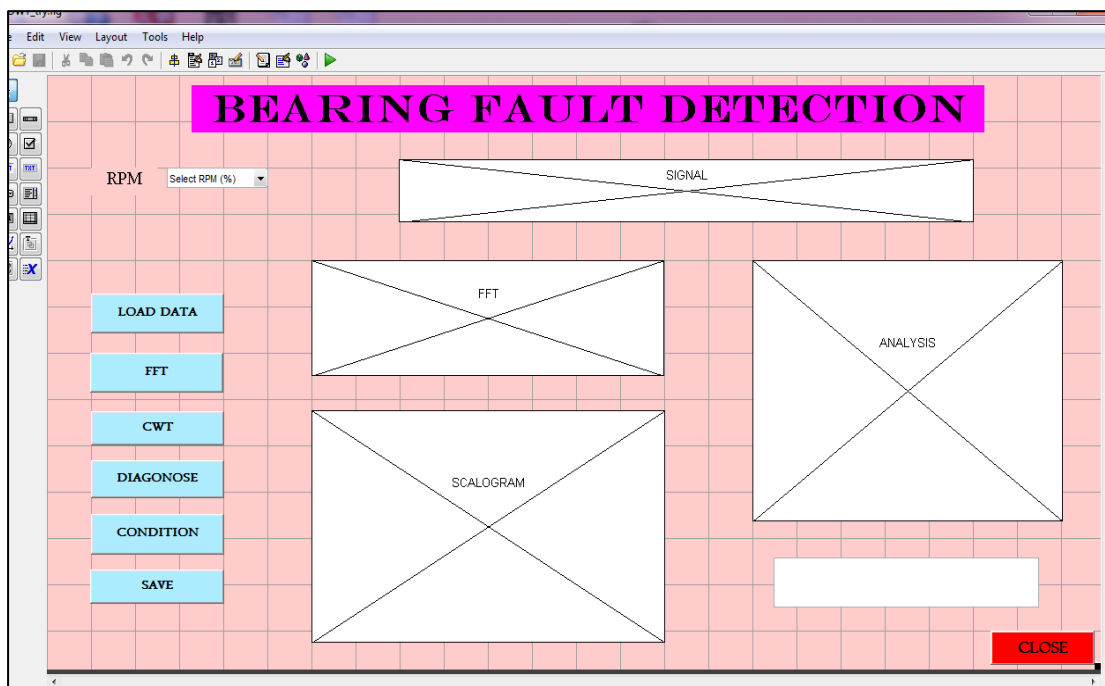


Figure 3.5: The complete layout of GUI

## CHAPTER 4

### RESULTS & DISCUSSION

#### 3.0 INTRODUCTION

This chapter presents the results and further discusses the outcome of the analysis. For the purpose of vibration signals collection, five groups of vibration signals were collected. Each of group is known as good bearing, contaminated bearing, inner race bearing, outer race bearing, and corroded bearing. Each group contains vibration signals of three level of speed which are 287 rpm as the lowest speed, 1,466 rpm as the medium speed, and 2,644 rpm as the highest speed.

#### 4.1 DATA

Figure 4.1 shows the vibration reading for the bearing running on 287 rpm with respect to each types of bearing defects and good bearing. Good bearing has the lowest amplitude as what you can expect from out of the box bearing with no defect. The outer race defect, the spike is more visible than the point defect even though the amplitude range is the same. Inner race defect has the quite same characteristic as the outer race defect but the amplitude range is more double from outer race defect due to spike are more intense than outer race defect.

While the contaminated defect result shows that the amplitude range are double than inner race defect, but it has even amplitude with small fraction of spikes. This is due to contaminated defect has debris all over inside the bearing. Lastly is the corroded defect which is you can see that the range of amplitude is same as contaminated but it is has more intensity spike all over the course of the graph. Contaminated and corroded can be said as had same characteristic but as corroded is the epitome of defect bearing and its intensity are what differentiate between the two.

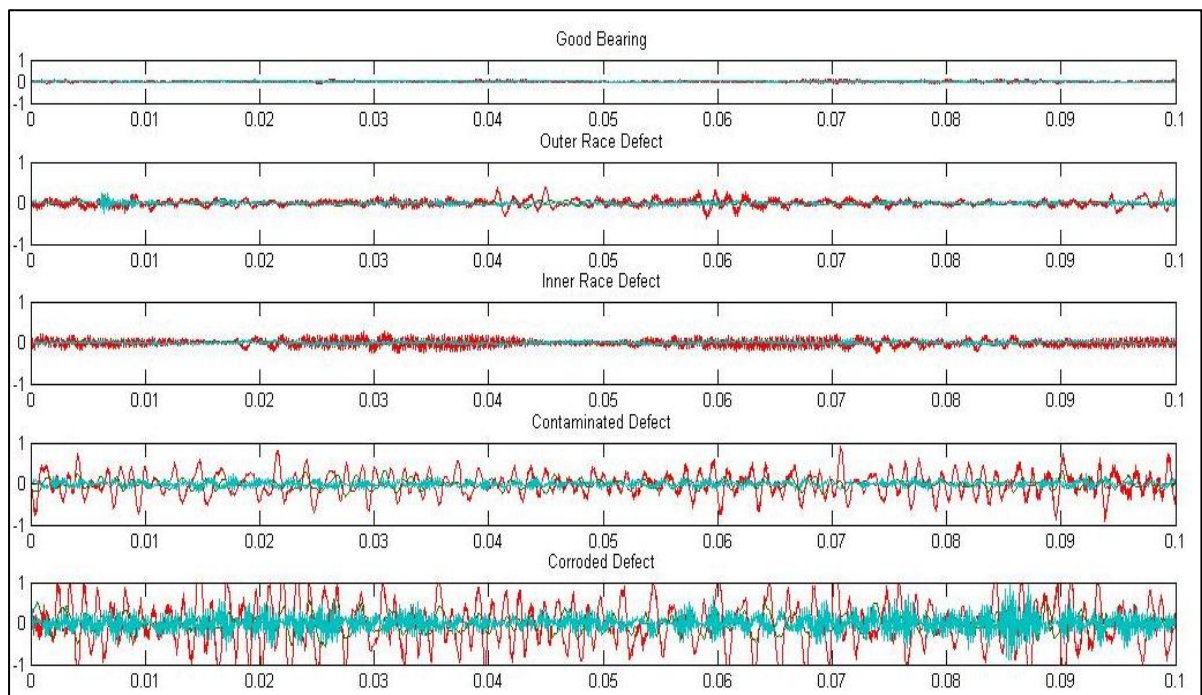


**Figure 4.1:** Vibration reading for the good condition of bearing on 287 rpm

In figure 4.2, good bearing graph of speed 1446 rpm show more or less the same as in 287 rpm. Here it has a uniform graph with a fraction of spikes. For outer race and inner race, the results conjured up is the same characteristic as in 287 rpm. The evenness of the graph for both and from the 287 rpm is more or less the same. But the spikes are much more frequent than earlier speed as more speed means more frequent rotation and more contact with the defect. So, the graph characteristic is the same as 287 rpm but due to speed increment, the spikes are more frequent.

For contaminated and corroded result also shows that they are much similar with the previous speed. The characteristic is the same but the amplitude range has increase more than tenfold than 287 rpm. The intensity of spikes is more toward corroded and then comes contaminated.

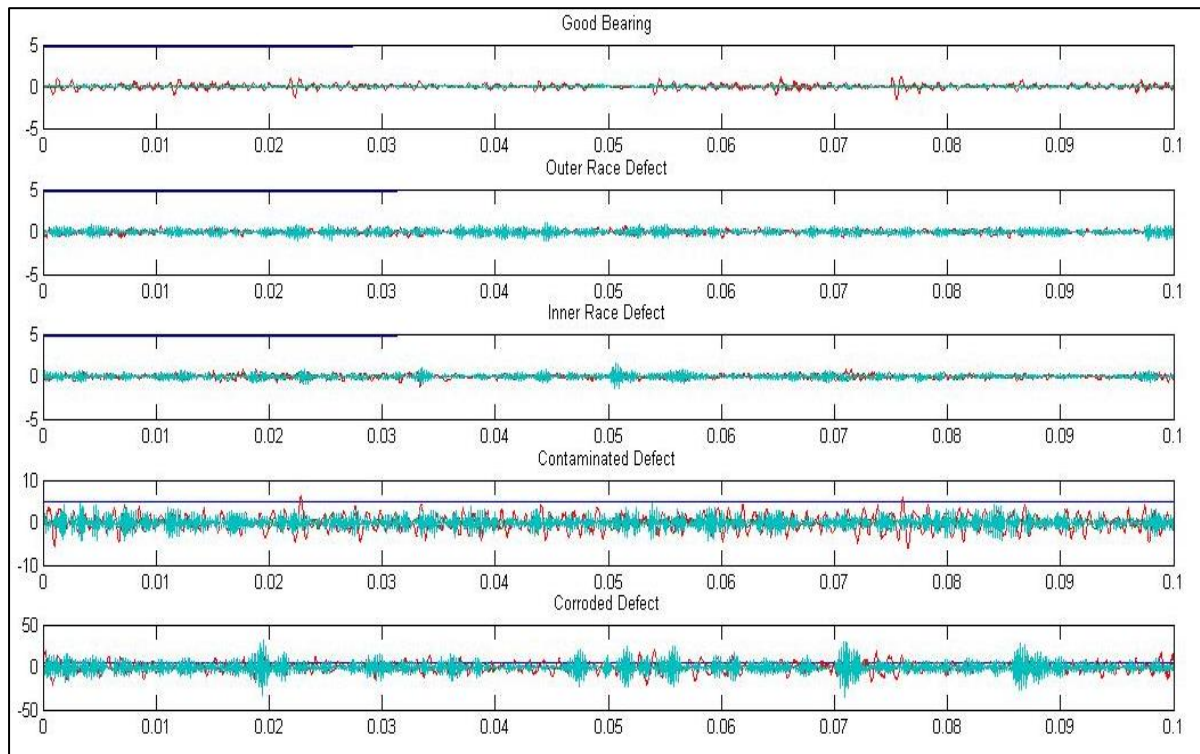


**Figure 4.2:** Vibration reading for the good condition of bearing on 1466 rpm

The entire characteristic discussed in the two previous speed usages also applied in 2664 rpm in figure 4.3. The entire graph has more frequent spikes due to higher speed results is more frequent rotation and frequent spikes due to higher speed result in more frequent contact with the defect area. Healthy has an even amplitude range with the small fraction of spikes.

In contaminated and corroded graph, the result is much the same as two previous graphs where the contaminated has increased its range and the spikes are everywhere. For corroded side view, the range has come up to a hundred, double from contaminated range. For outer race and inner race defect, the visible spikes on both of them as you can

see in the 287 rpm have become a part of the graph due to the increased speed. But, in this speed the inner race have much more higher amplitude of the graph than outer race.

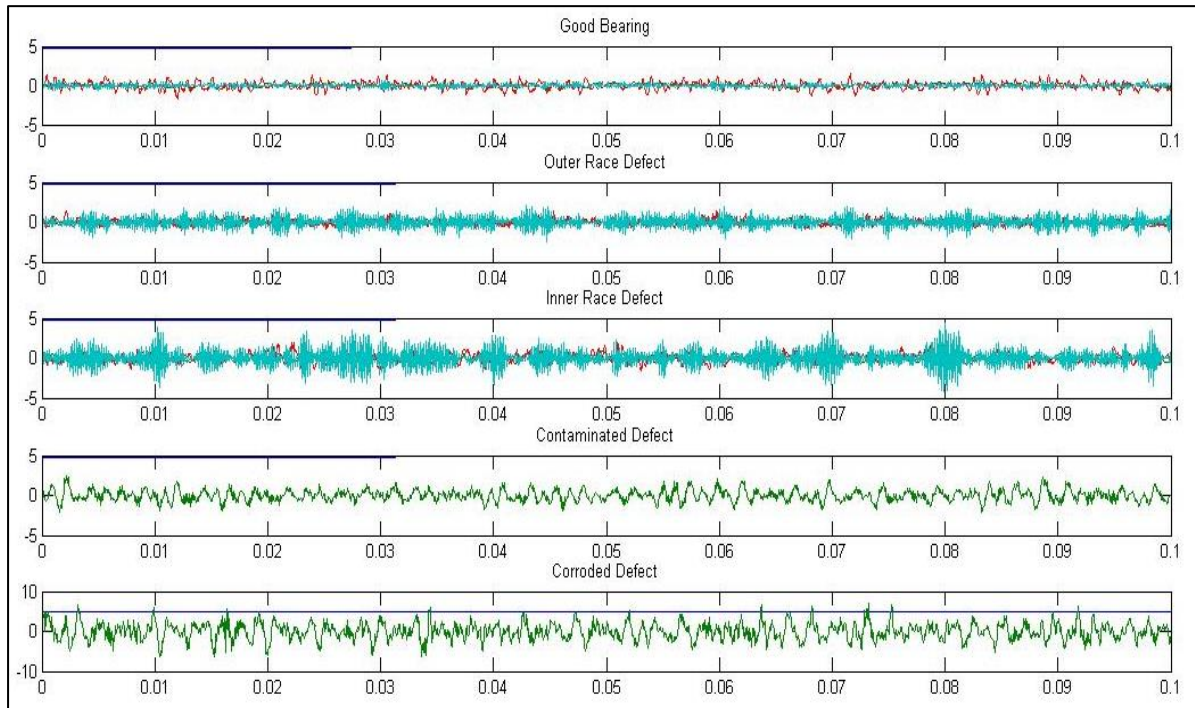


**Figure 4.3:** Vibration reading for the good condition of bearing on 2664 rpm

## 4.2 SCALOGRAM RESULT

Figure 4.4 to Figure 4.21 shows the time domain and the wavelet analysis scalogram for all type of tested bearing including the good ones at three different speed. The magnitude of the CWT is called the scalogram. We can make 2 dimensional plots of the scalogram with time on the horizontal axis, scale on the vertical axis, and amplitude given by a gray-scale colour. The continuous wavelet transform decomposes a signal into a series of time-varying coefficients. The wavelet scalogram plots the magnitude of these coefficients by representing each coefficient as a single row. The scalogram is a time-varying spectral representation of the signal. It also represents the percentage of energy for each coefficient. Next, the time domain data will be transforming into time-frequency domain which is scalogram wavelet coefficient transform. To obtain that, a coding had been used into software that is already



formulated in the software. The scalogram wavelet transform consist a wavelet coefficients data the data had been extract out means by that only at that area the wavelet coefficient will be count. The wavelet coefficient data at the frequency range had been sum to get the total coefficient value at the point of location. The process had been done to all the type of defect and the good bearing.

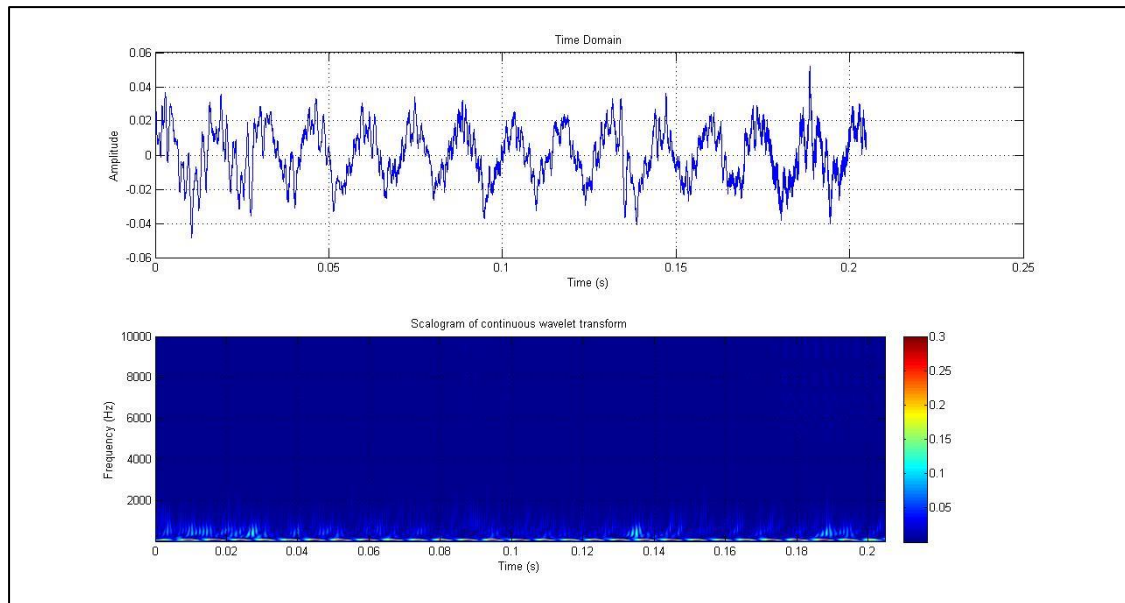


**Figure 4.4:** Time domain for the good condition of bearing on 287 rpm and scalogram of wavelet analysis

From the result generated, detectable defect feature obviously appears from corroded bearing at 2664 rpm by seeing the energy coefficient increased. Some result of coefficient to be weakly observed throughout the energy for speed 287 rpm and 1466 rpm especially at inner race defect. The others defects clearly seen the energy of coefficient can be observed.

This shows that CWT be efficient for online monitoring method when there's enough frequency excitation by applying CWT on a system running on high speed of at least 2664 rpm.



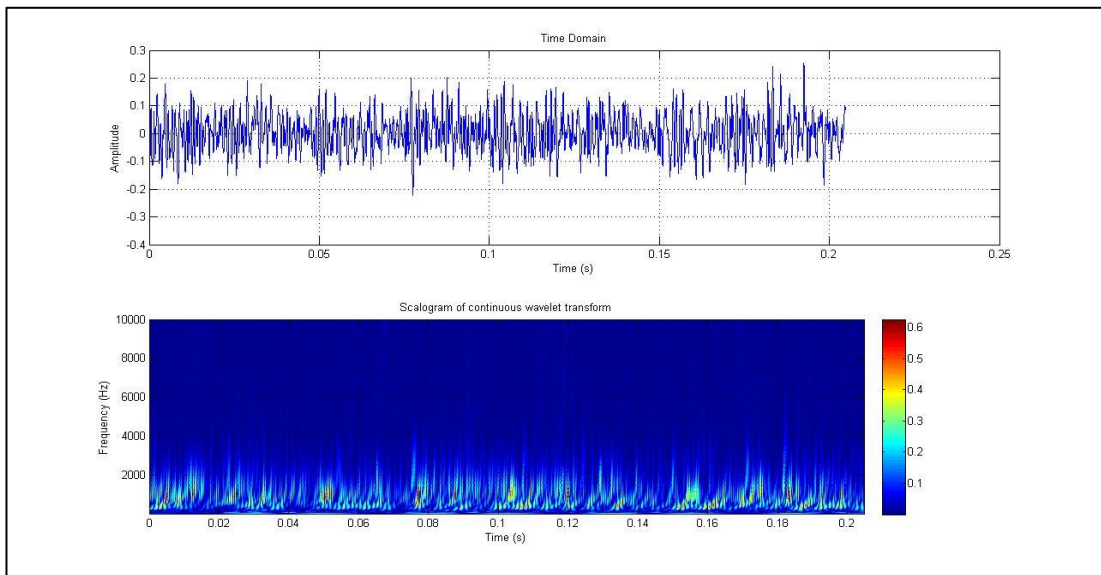


**Figure 4.5:** Time domain for the good condition of bearing on 1466 rpm and scalogram of wavelet analysis

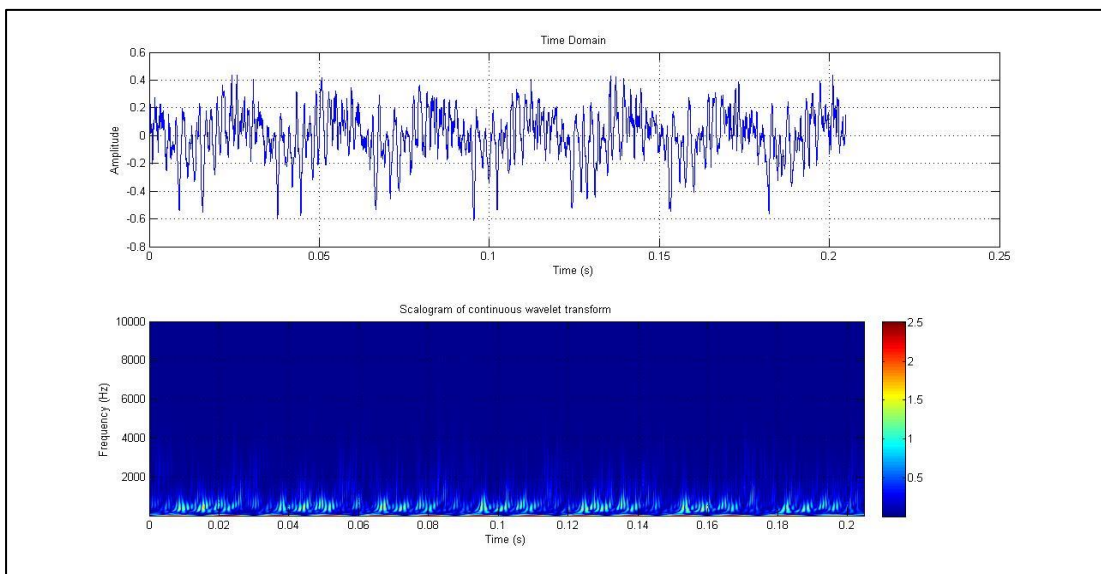


**Figure 4.6:** Time domain for the good condition of bearing on 2664 rpm and scalogram of wavelet analysis

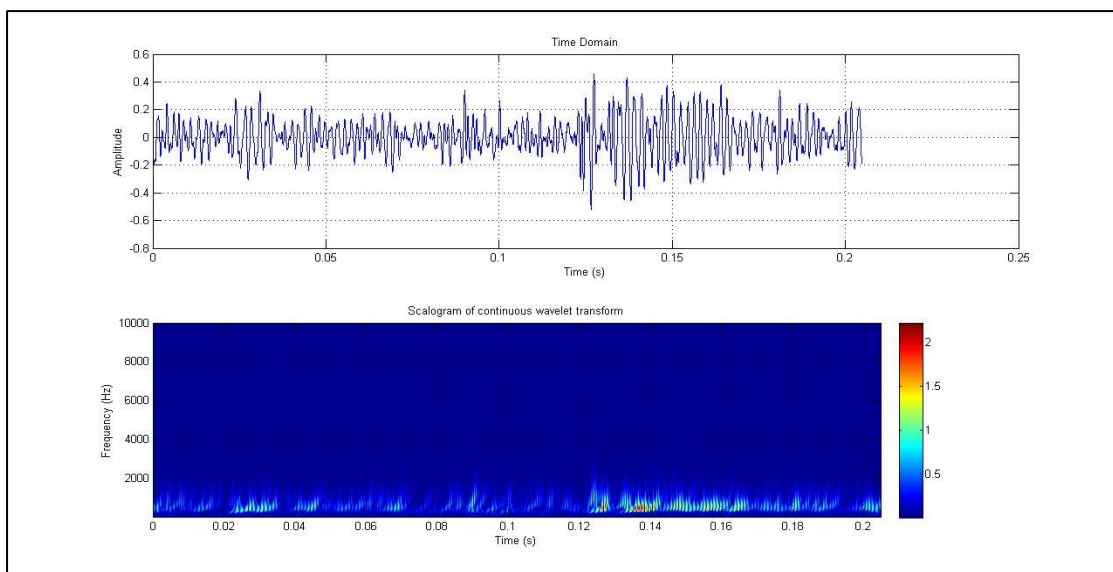


**Figure 4.7:** Time domain for the contaminated defect on 287 rpm and scalogram of wavelet analysis

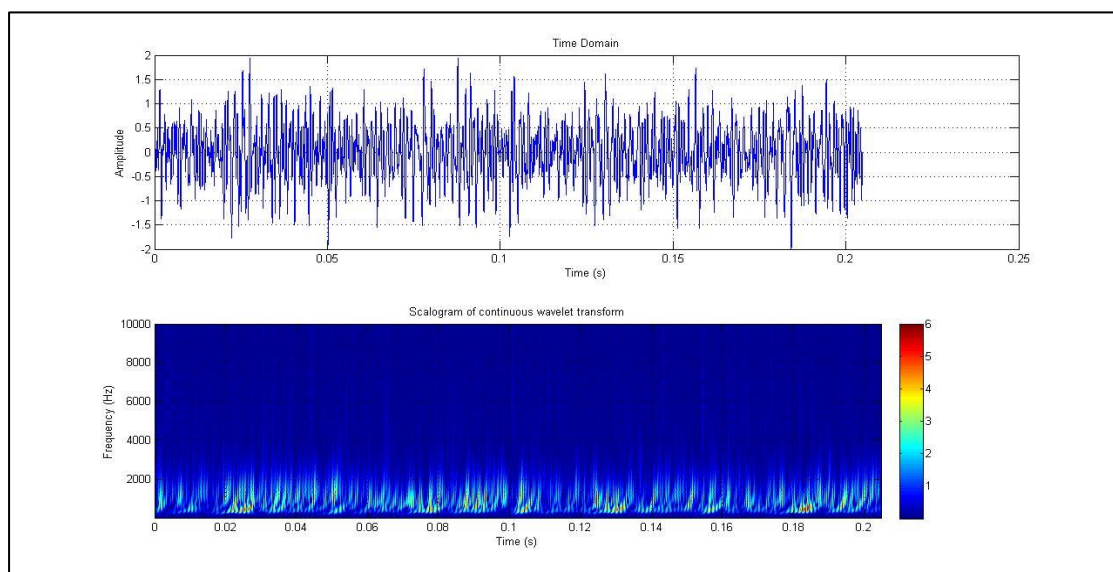


**Figure 4.8:** Time domain for the contaminated defect on 1466rpm and scalogram of wavelet analysis

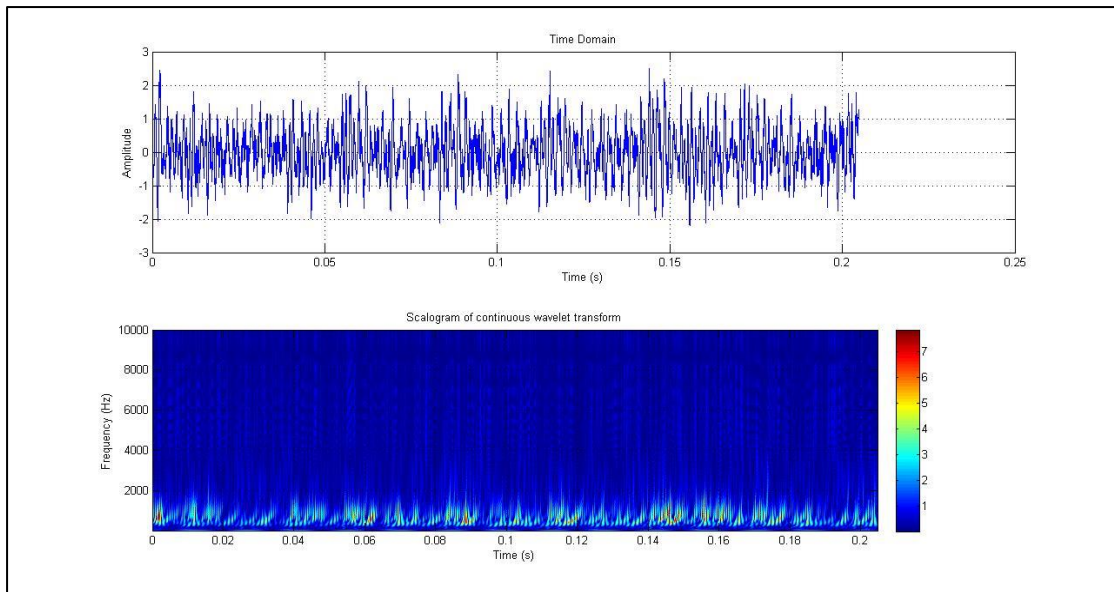


**Figure 4.9:** Time domain for the contaminated defect on 2664 rpm and scalogram of wavelet analysis

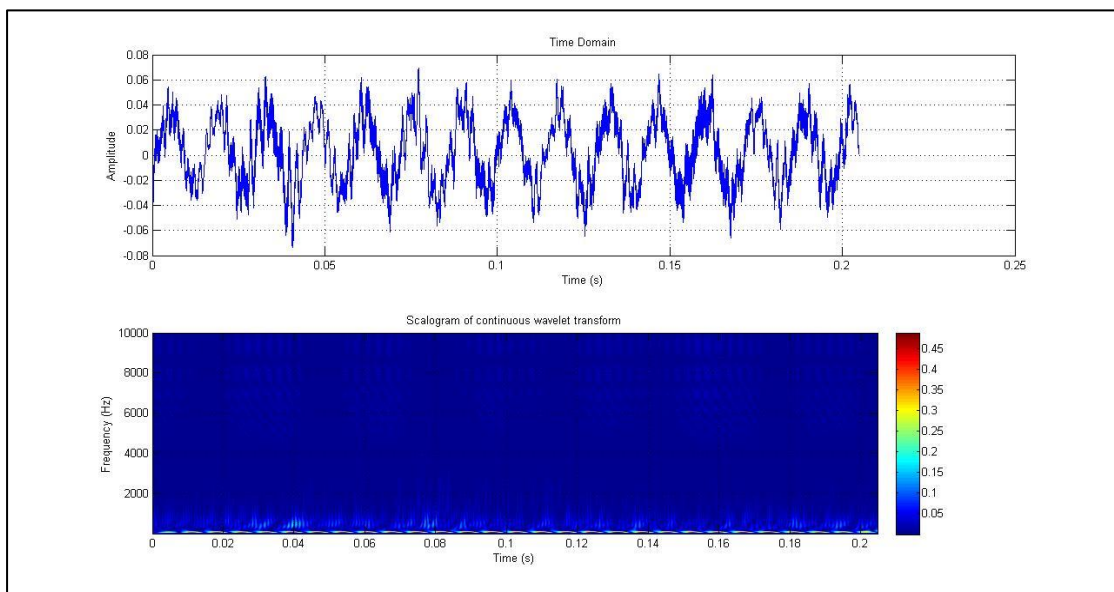


**Figure 4.10:** Time domain for the inner race defect on 287 rpm and scalogram of wavelet analysis

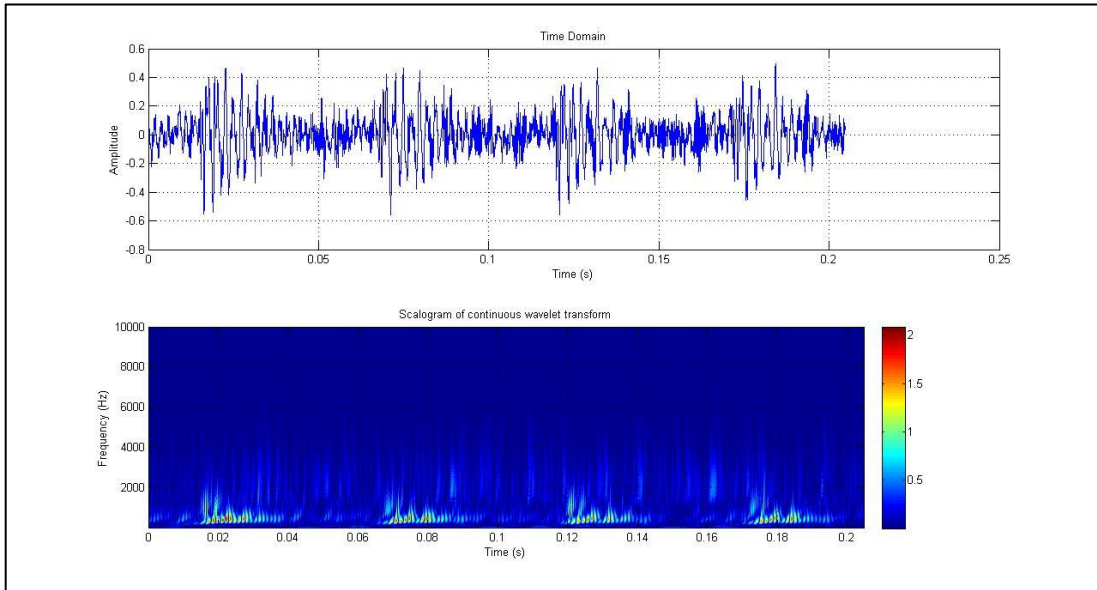


**Figure 4.11:** Time domain for the inner race defect on 1466 rpm and scalogram of wavelet analysis

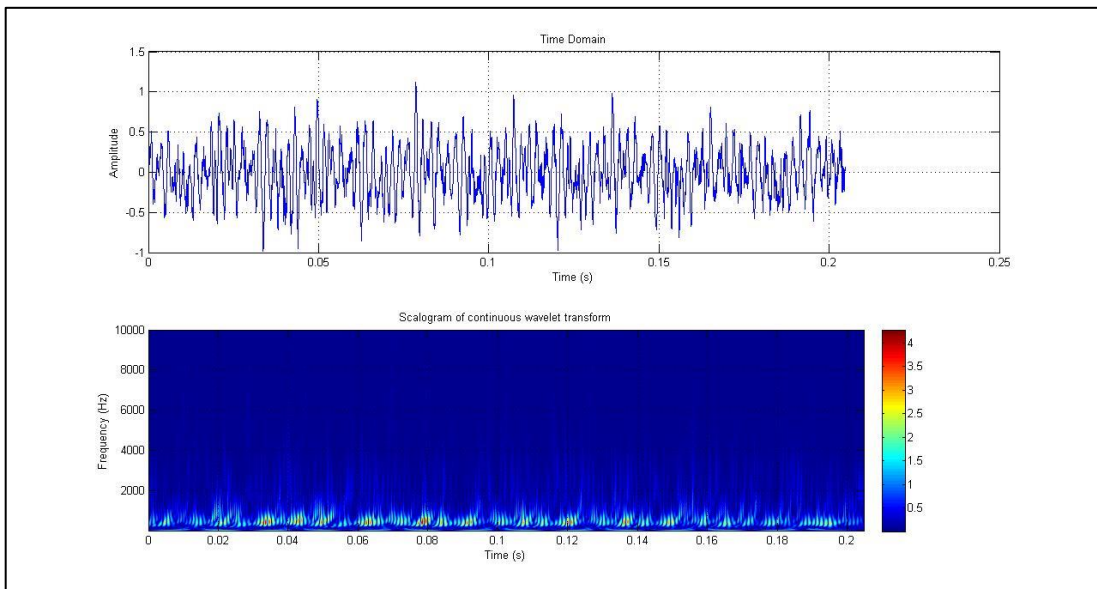


**Figure 4.12:** Time domain for the inner race defect on 2664 rpm and scalogram of wavelet analysis

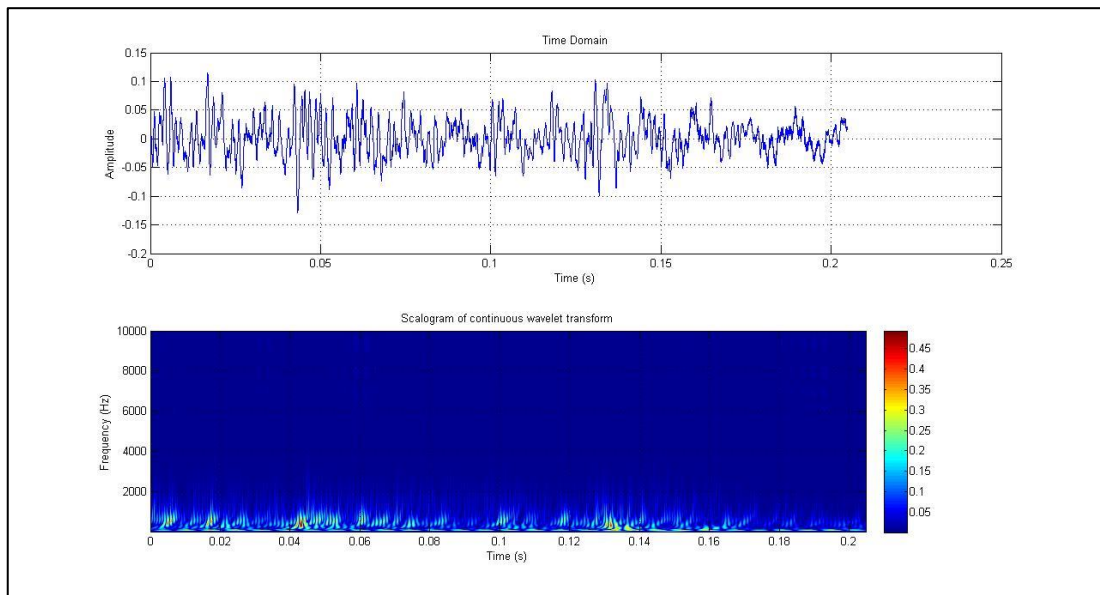


**Figure 4.13:** Time domain for the outer race defect on 287 rpm and scalogram of wavelet analysis

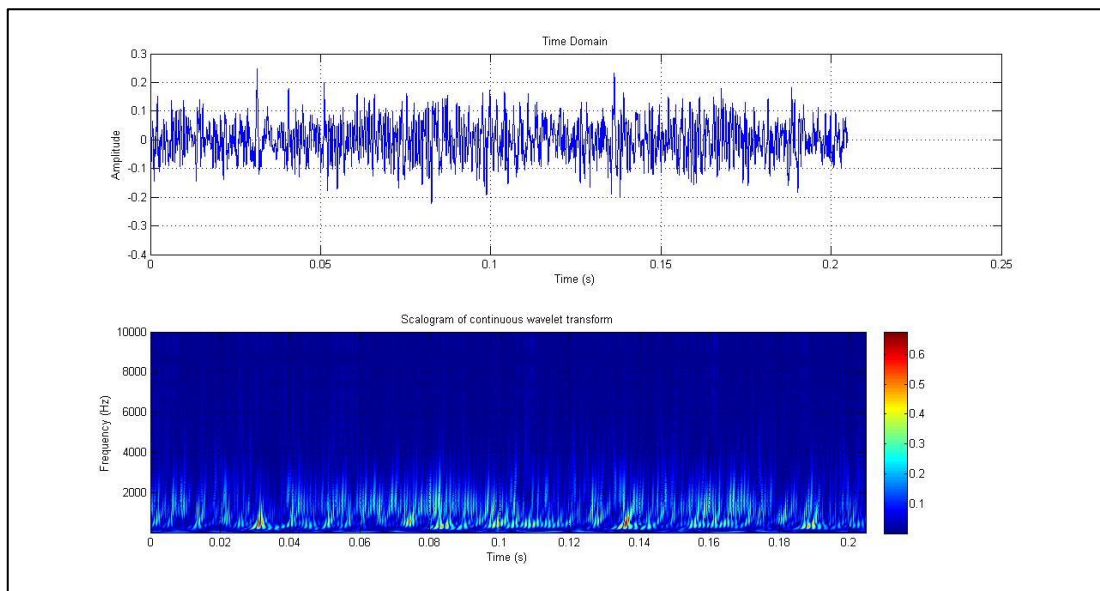


**Figure 4.14:** Time domain for the outer race defect on 1466rpm and scalogram of wavelet analysis



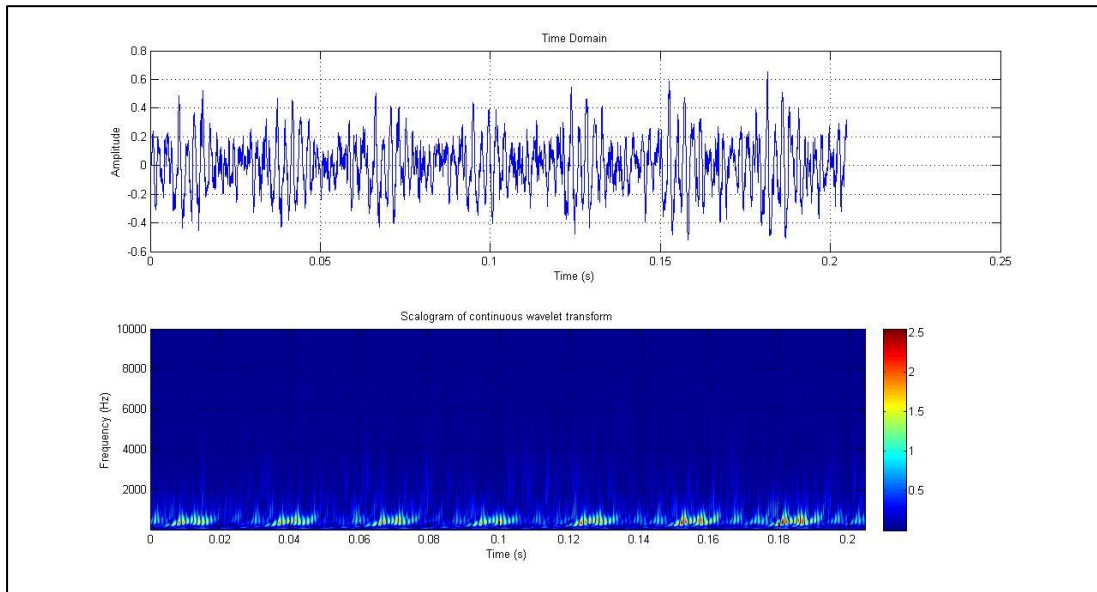


**Figure 4.15:** Time domain for the outer race defect on 2664 rpm and scalogram of wavelet analysis

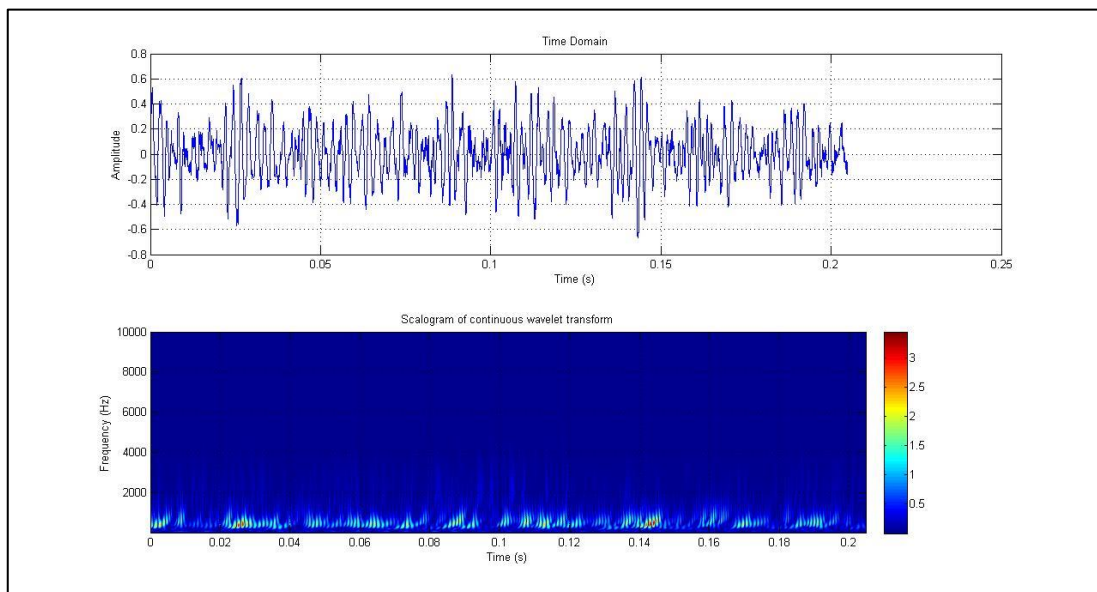


**Figure 4.16:** Time domain for the corroded defect on 287 rpm and scalogram of wavelet analysis

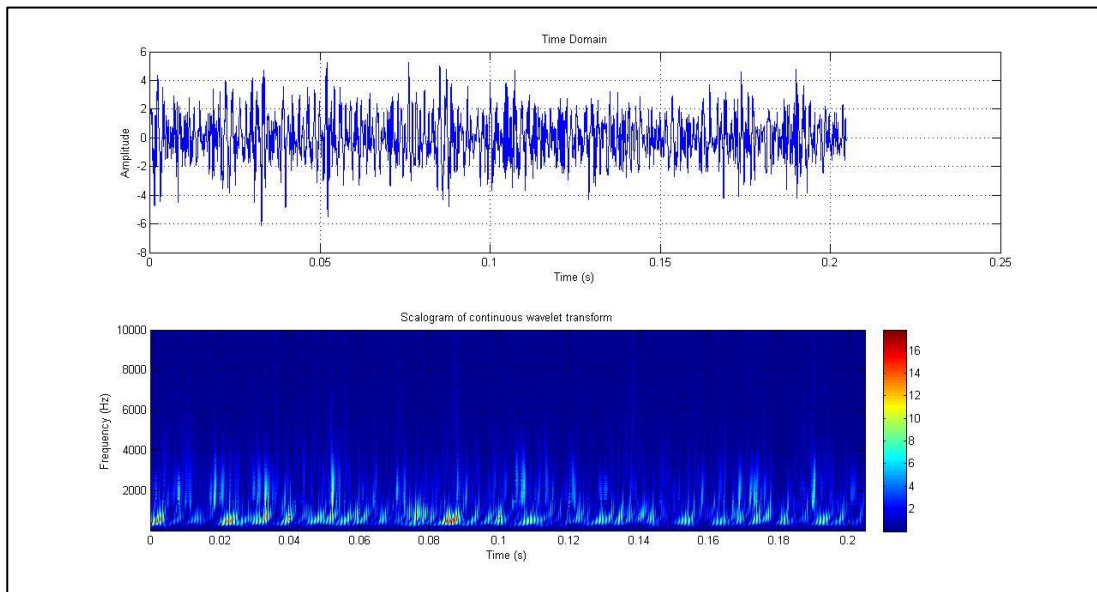


**Figure 4.17:** Time domain for the corroded defect on 1466 rpm and scalogram of wavelet analysis

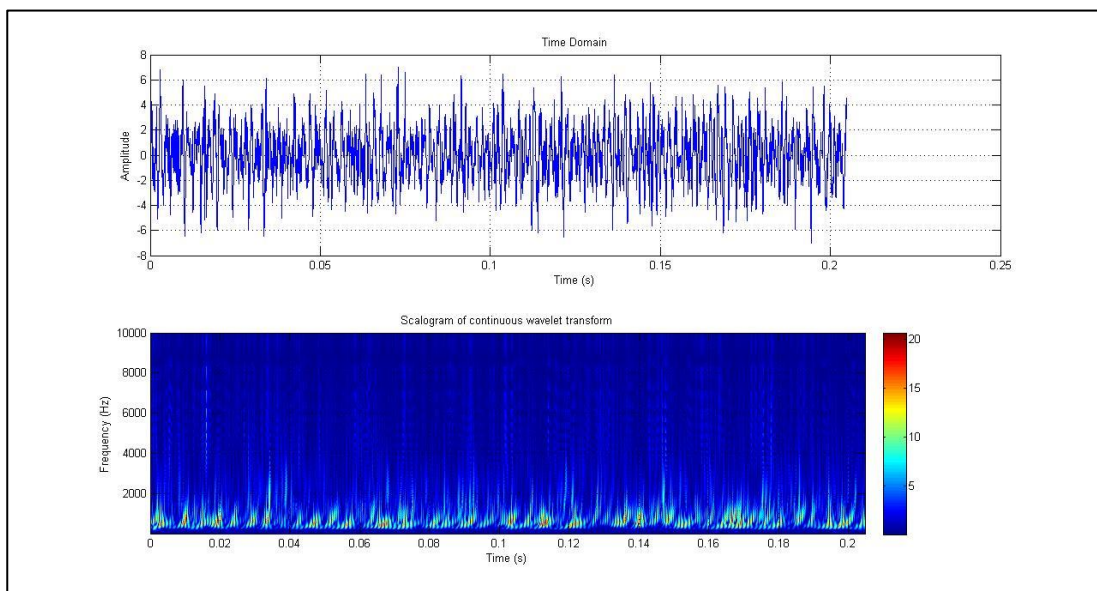


**Figure 4.18:** Time domain for the corroded defect on 2664 rpm and scalogram of wavelet analysis

### 4.3 WAVELET COEFFICIENT ANALYSIS

For data of insufficient frequency excitation, calculating the wavelet coefficient value for each level seems to yield understandable trend when graph is plotted. The coefficient is a multiplicative factor in some term of an expression or of a series. It is usually a number, but in any case does not involve any variables of the expression. Any value of wavelet coefficient or graph plotted that is below the good line may be considered defected. This is because the decomposition process is where the frequency amount of each level gets smaller as the decomposition level increases. So, if the wavelet coefficient of the next level declines at an irregular rate or stays flat on its line, the bearing may be considered as defected.

#### 4.3.1 Wavelet Coefficient for 287 rpm

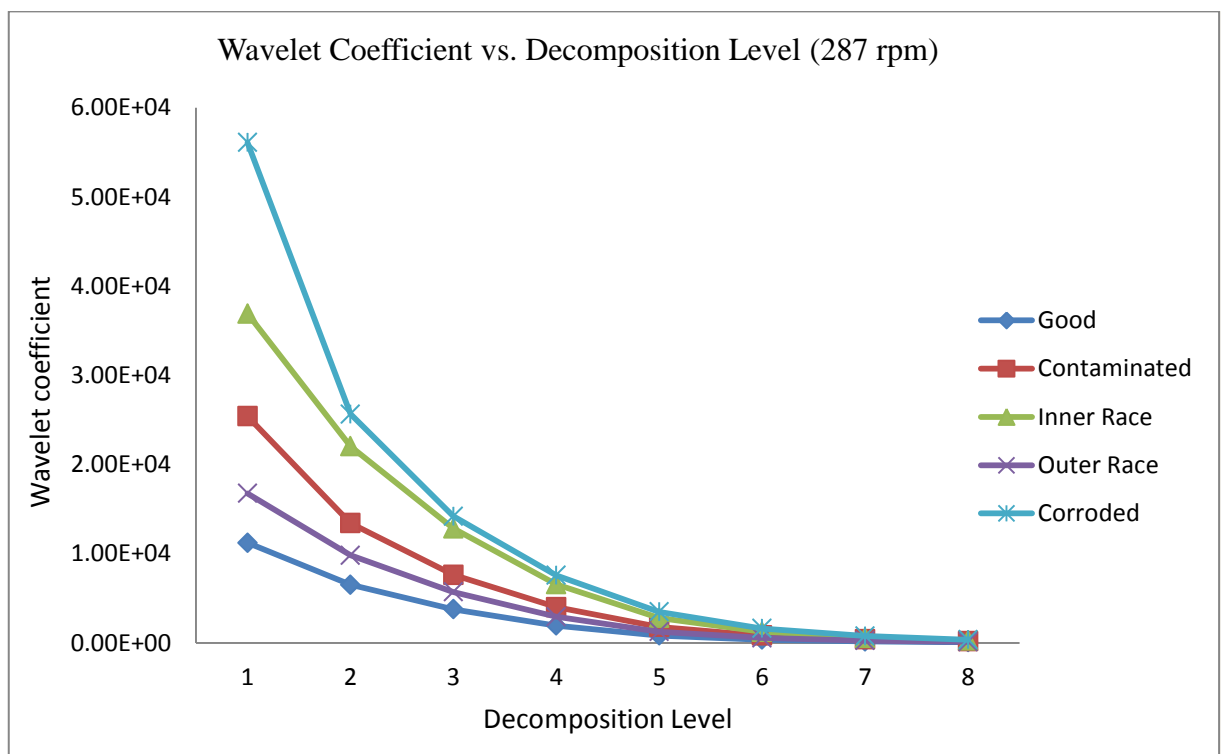
Table 4.1 shows the value of wavelet coefficient for each level of decomposition for data of 287 rpm. From the data, the wavelet coefficient of the defected bearing is higher than the good one. It also shows that the wavelet coefficient of seriously defect such as contaminated and corroded defect are had high different to another defect and the good bearing itself. So, the wavelet coefficient will high if there is defect occur in the bearing.

Figure 4.19 shows the trend generated by the wavelet coefficient value of each decomposition level. From the plotted graph, the defect wavelet coefficient value for each decomposition level is over from the good line. So, it can say that if the wavelet coefficients of the bearing are in this condition, the bearing are probably had a defect.



**Table 4.1:** Wavelet coefficient value for each level decomposition at 287 rpm

D. Level	Wavelet Coefficient				
	Good	Inner Race Defect	Outer Race Defect	Corroded	Contaminated
1	11214.11	36922.12	16770.04	56105.03	25405.01
2	6518.4	22045.02	9819.31	25654.12	13430.31
3	3770.01	12825.21	5697.52	14188.11	7626.42
4	1938.21	6565.03	2924.74	7568.32	4002.21
5	830.04	2795.84	1253.12	3482.13	1801.54
6	366.06	1228.43	553.56	1621.84	832.38
7	167.58	561.07	253.63	764.74	390.76
8	77.88	260.39	117.91	360.92	183.92

**Figure 4.19:** Wavelet coefficient vs. decomposition level for speed at 287 rpm

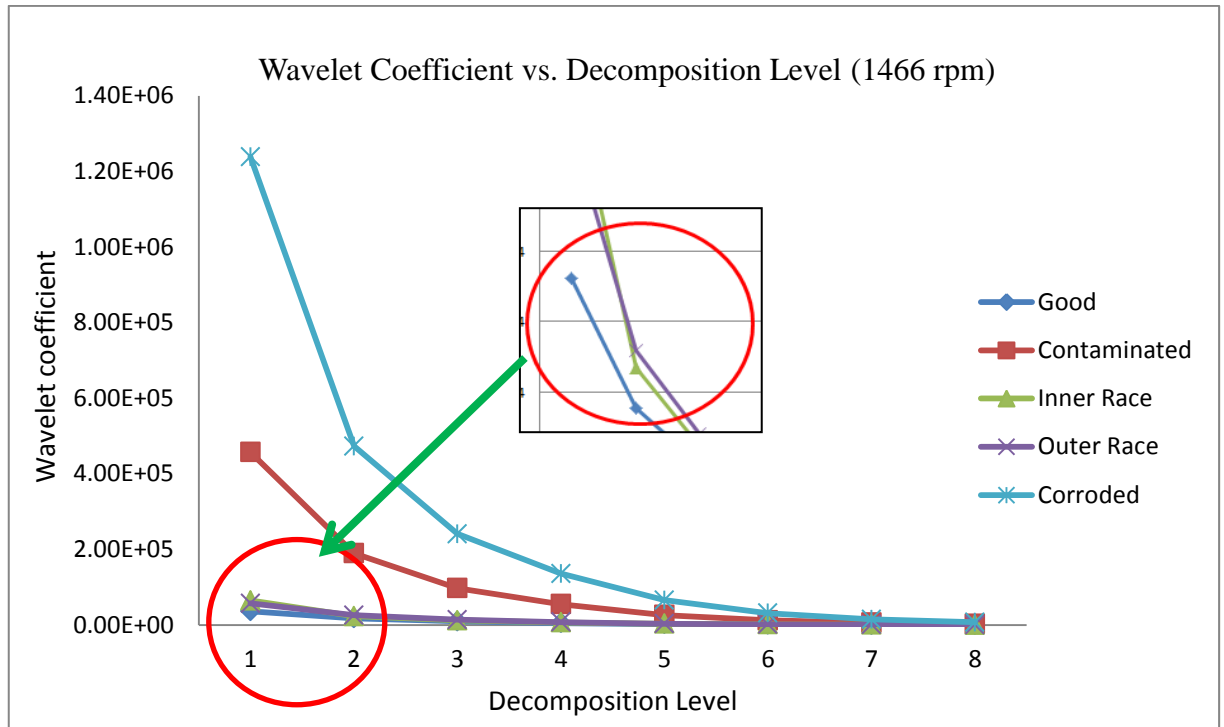
### 4.3.2 Wavelet Coefficient for 1466 rpm

Table 4.2 shows the value of wavelet coefficient for each level of decomposition for data of 1466 rpm. The wavelet coefficient in this speed is increasing from the lower speed running, 287 rpm. It shows that the wavelet coefficient of seriously defect such as contaminated and corroded defect are higher than to another defect and the good bearing itself. So, the wavelet coefficient will high if there is defect occur in the bearing

Figure 4.20 shows the trend generated by the wavelet coefficient value of each decomposition level. From the plotted graph, it seems that all the defected bearing's wavelet coefficient value for each decomposition level is upper the good line. But the corroded and contaminated are more further from the good one compare to another defect.

**Table 4.2:** Wavelet coefficient value for each level decomposition at 1466 rpm

D. Level	Wavelet Coefficient				
	Good	Inner Race Defect	Outer Race Defect	Corroded	Contaminated
1	3.62E+04	6.49E+04	5.72E+04	1.24E+06	4.57E+05
2	1.76E+04	2.34E+04	2.59E+04	4.73E+05	1.90E+05
3	9.79E+03	1.23E+04	1.40E+04	2.41E+05	9.75E+04
4	5.22E+03	6.82E+03	7.58E+03	1.36E+05	5.50E+04
5	2.36E+03	3.38E+03	3.46E+03	6.57E+04	2.60E+04
6	1.09E+03	1.64E+03	1.60E+03	3.12E+04	1.21E+04
7	508.9334	792.5333	751.1396	1.49E+04	5.79E+03
8	239.4765	378.2598	354.1097	7.09E+03	2.74E+03



**Figure 4.20:** Wavelet coefficient vs. decomposition level for speed at 1466 rpm

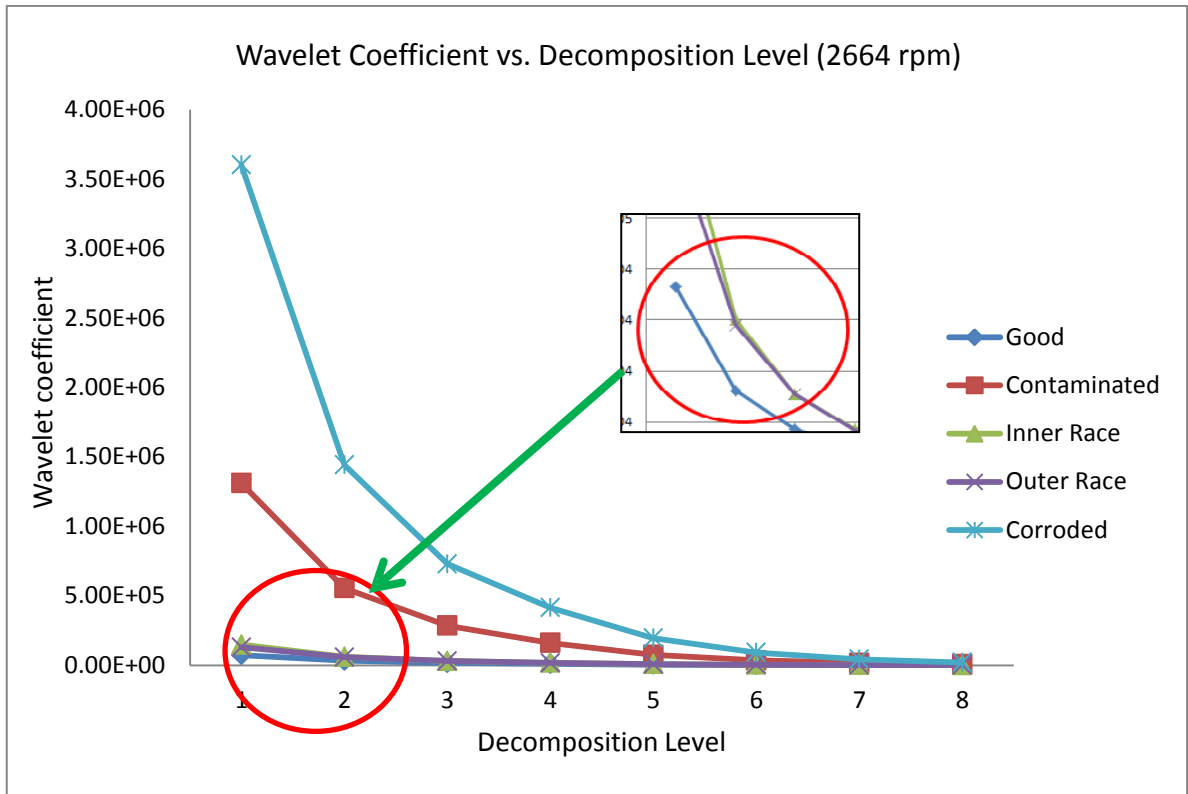
### 4.3.3 Wavelet Coefficient for 2664 rpm

Table 4.3 shows the value of wavelet coefficient for each level of decomposition for data of 2664 rpm. The wavelet coefficient in this speed is increasing from the lower speed running, 287 rpm and 1466 rpm. The higher wavelet coefficient refers to the serious damage which is corroded and contaminated defect while the inner and outer race defects are still had higher wavelet coefficient than the good bearing. So, the wavelet coefficient can act as an indicator to determine either the bearing is in good condition or not.

**Table 4.3:** Wavelet coefficient value for each level decomposition at 2664 rpm

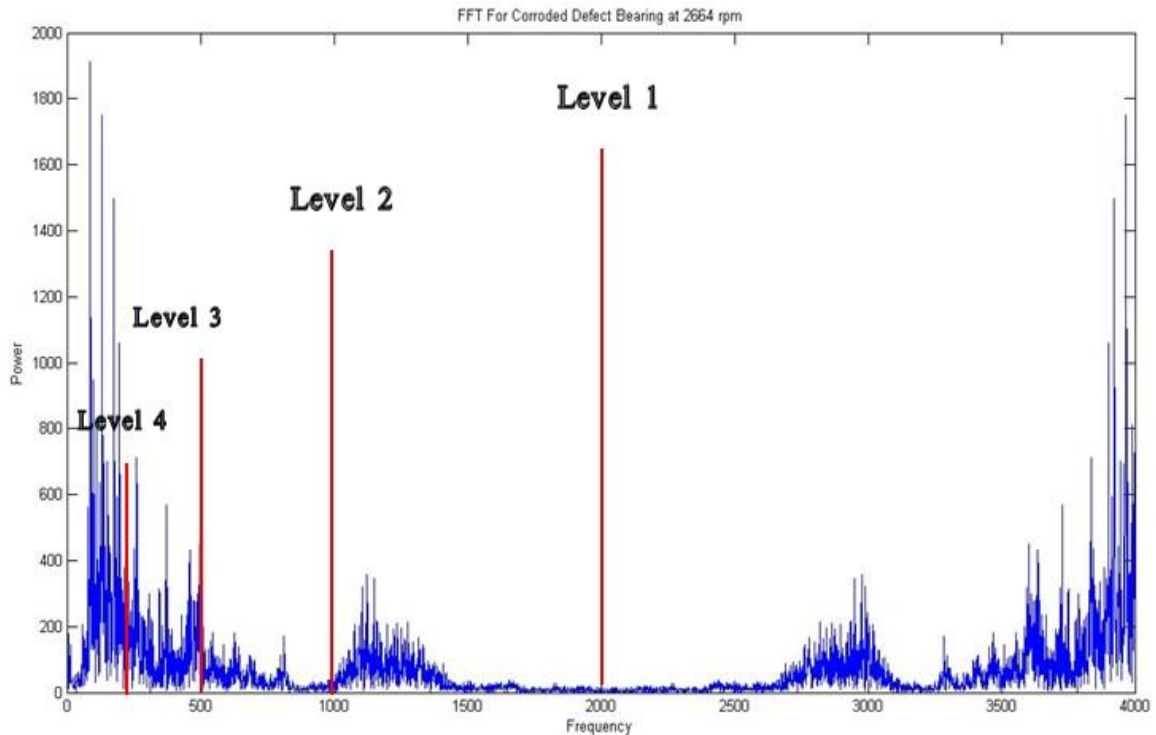
<b>D.</b> Level	<b>Wavelet Coefficient</b>				
	<b>Good</b>	<b>Inner Race Defect</b>	<b>Outer Race Defect</b>	<b>Corroded</b>	<b>Contaminated</b>
<b>1</b>	7.32E+04	1.48E+05	1.29E+05	3.60E+06	1.31E+06
<b>2</b>	3.23E+04	6.00E+04	5.80E+04	1.44E+06	5.54E+05
<b>3</b>	1.72E+04	3.10E+04	3.10E+04	7.29E+05	2.86E+05
<b>4</b>	9.45E+03	1.74E+04	1.69E+04	4.14E+05	1.60E+05
<b>5</b>	4.37E+03	8.27E+03	7.76E+03	1.96E+05	7.47E+04
<b>6</b>	2.03E+03	3.90E+03	3.57E+03	9.15E+04	3.46E+04
<b>7</b>	9.57E+02	1.85E+03	1.68E+03	4.34E+04	1.63E+04
<b>8</b>	4.52E+02	877.8533	789.8878	2.05E+04	7.72E+03

Figure 4.21 shows the trend generated by the wavelet coefficient value of each decomposition level. From the plotted graph, it seems that all the defected bearing's wavelet coefficient value for each decomposition level is upper the good line. This graph shows that the wavelet coefficient for corroded and contaminated defect had more further from the good bearing while the inner and outer race defect are still close to the reference line. It can say that the more serious defect will be obtained if the wavelet coefficient itself are more slightly further away from the reference line but the minor defect still can be obtained if the wavelet coefficient are still higher than the good one. So, the further gap between the good one, it most probably had the serious damage on the bearing.



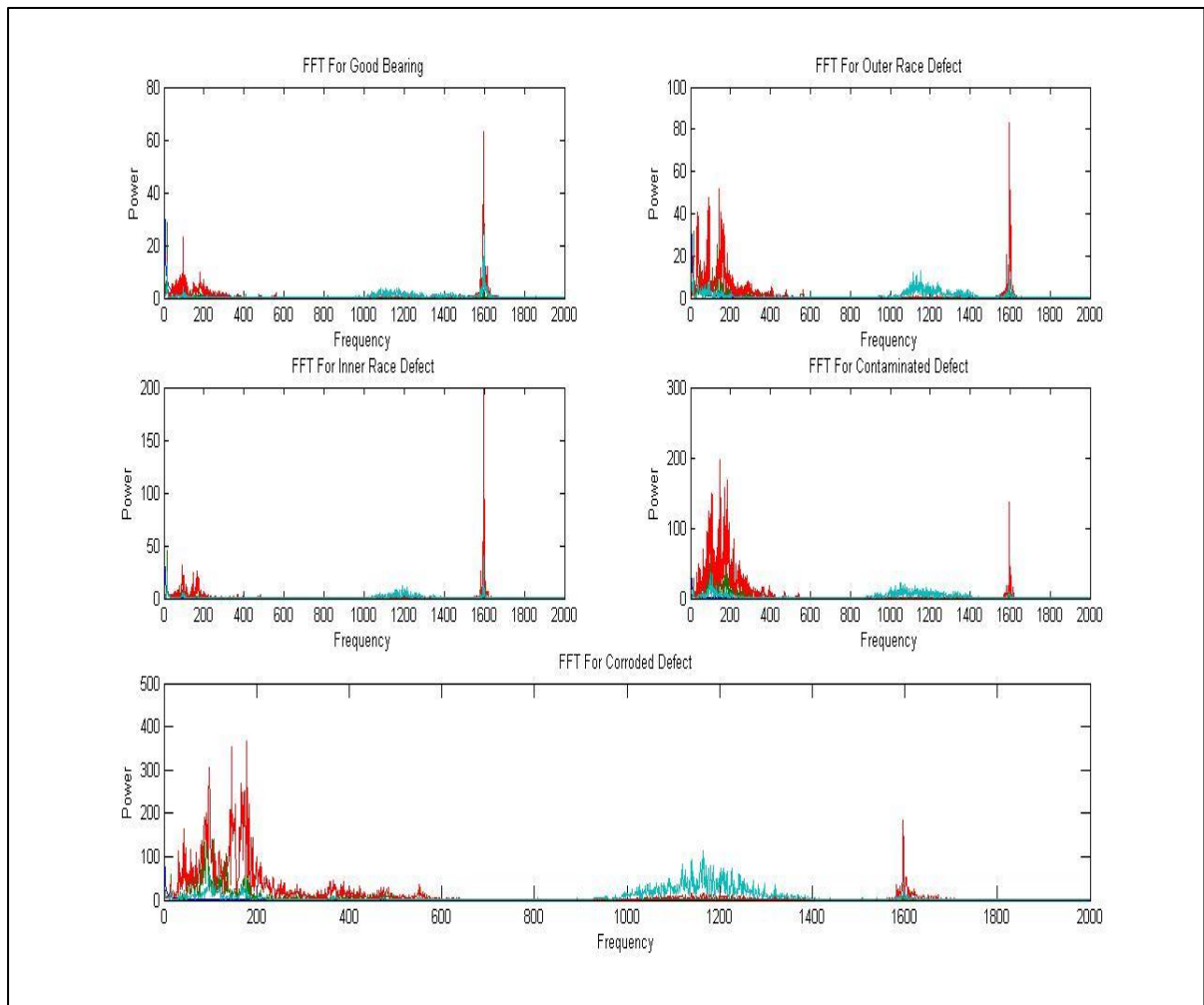
**Figure 4.21:** Wavelet coefficient vs. level decomposition for speed at 2664 rpm

Most information of a signal is often carried by the singularity points, such as the peaks, the discontinuities, etc. Moreover, at the moment when faults occur, the output signals usually contain jump points that often are singularity points. Therefore, singularity detection has played an important role in fault diagnostics. The polynomial trends in the signals could mask the local weak singularities in signals and this caused some methods failing to detect those singularities. On the other hand, the wavelet function can be chosen as the orthogonal to polynomial behaviour of arbitrarily high order, and therefore can remove the polynomial trends and highlight the singularity points in signals, thus the singularity points can be detected easily by the wavelet-based methods. In Figure 4.22 shown the FFT graph for corroded ball bearing condition on 2664 rpm and the way how to divide the level for calculate the wavelet of coefficient.



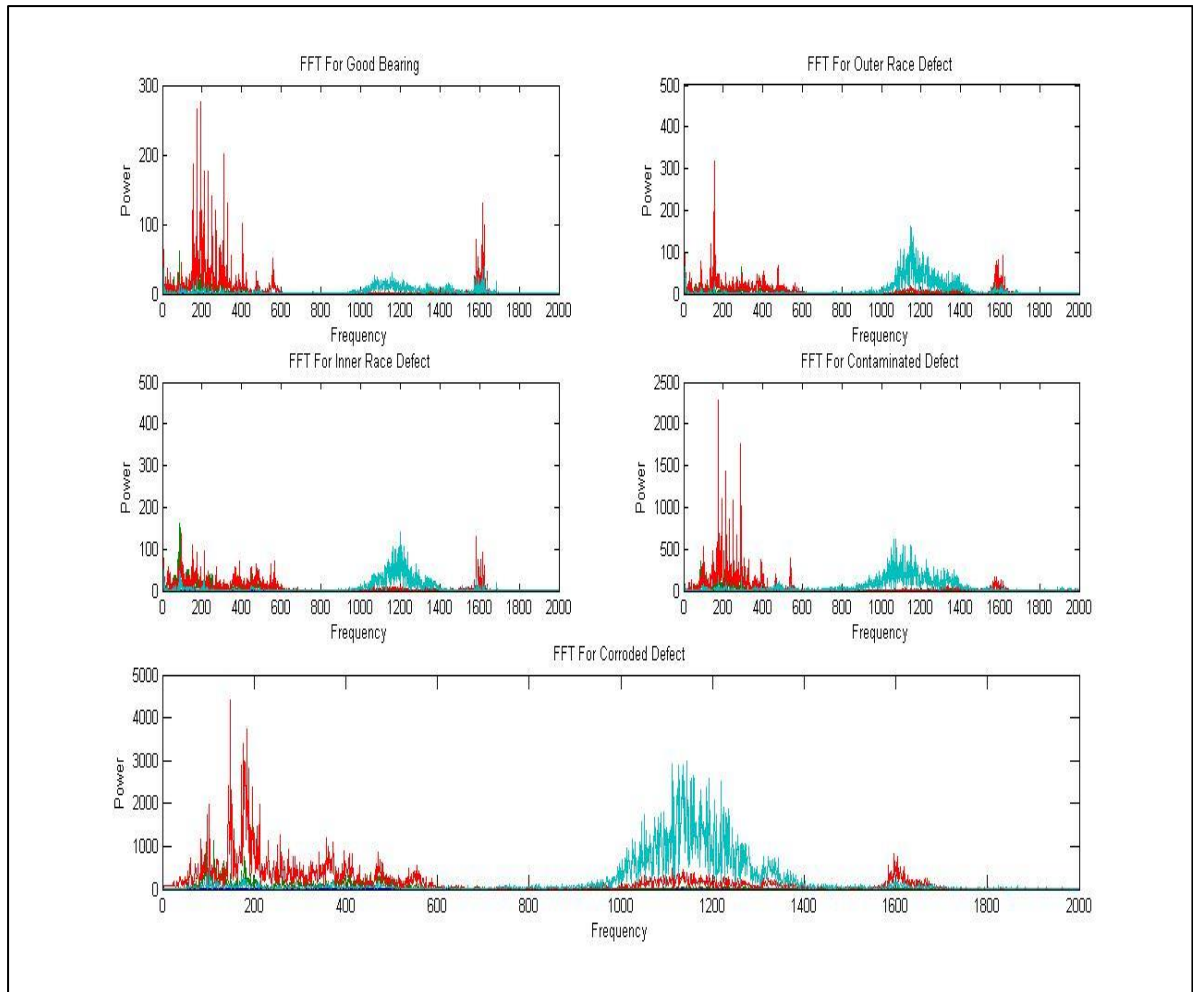
**Figure 4.22:** FFT result for corroded ball defect at 2664 rpm.

Figure 4.23 shows the FFT graph at running speed 287 rpm for all types of bearing and the good one. From the graph, it shows that there is obviously appear another high peak of amplitude at the middle of the signal for defected bearing. According the figure it shows that the defected bearing has their own characteristic itself and it will affected signal due to the types of defect. The amplitude of another peak of defected bearing are depend of the serious level of damage of the bearing itself. The more serious defect such as corroded and contaminated, the amplitude will be more high compare to the minor defect such as inner and outer race.



**Figure 4.23:** FFT graph for bearing at 287 rpm

Figure 4.24 shows the FFT graph at running speed 1466 rpm for all types of bearing and the good one. The amplitude of another peak of defected bearing is obviously appear and had high amplitude compare to the running speed at 287 rpm. It shows that the amplitude of defected bearing will increase due the increasing of the speed running of machine. So, the defected of bearing are much easier to detect in the high speed.



**Figure 4.24:** FFT graph for bearing at 1466 rpm

Figure 4.25 shows the FFT graph at running speed 2664 rpm. The amplitude of another peak of defected bearing is obviously appear and had high amplitude compare to the running speed at 1466 rpm and 287 rpm even though in the minor defect which is inner and outer race. It shows that the amplitude of defected bearing will increase due the increasing of the speed running of machine. So, the defected of bearing can be observed on the FFT graph and it more easier detect the defect occurring in the bearing at the high speed.



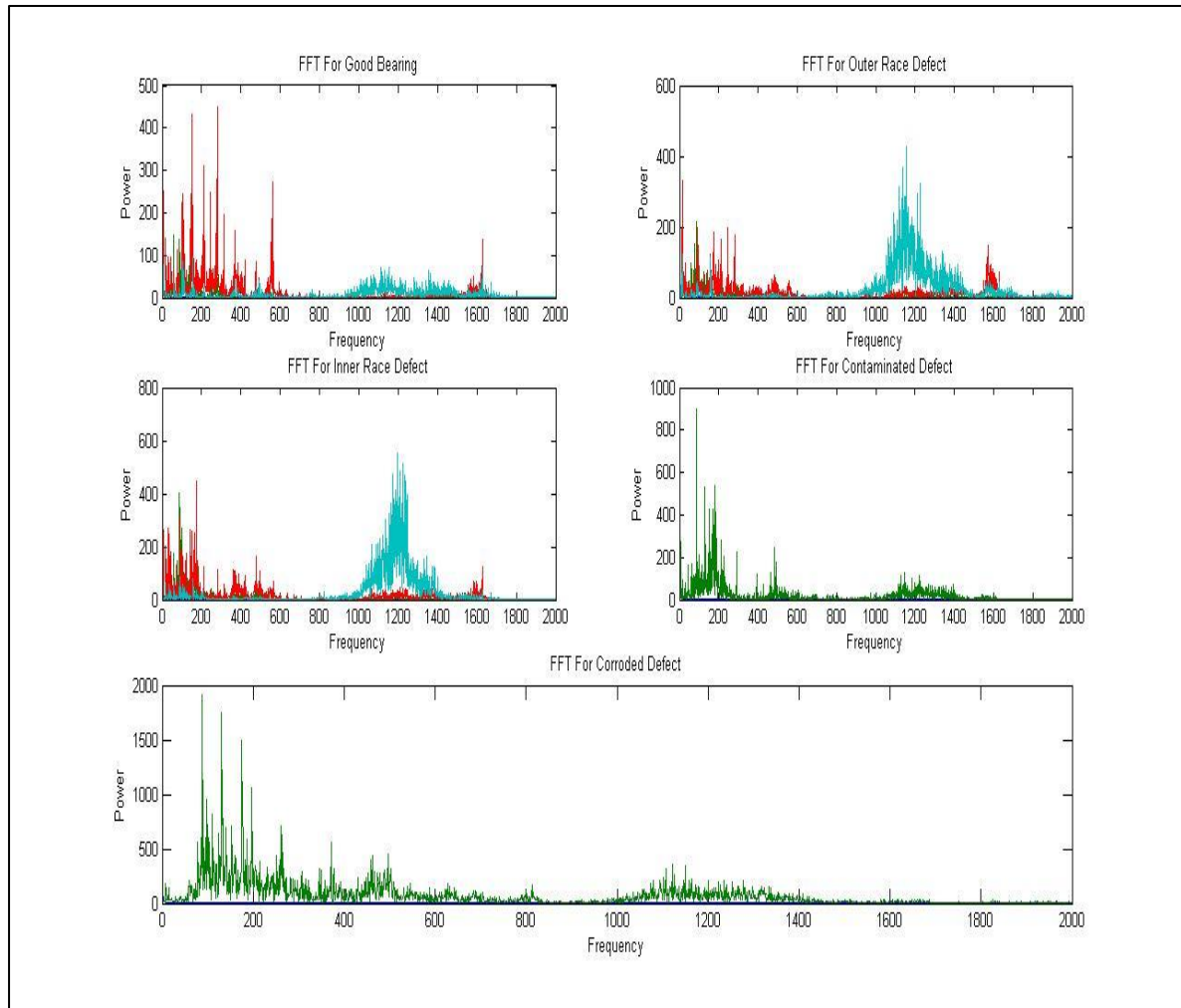


**Figure 4.25:** FFT graph for bearing at 2664 rpm

#### 4.4 GRAPHICAL USER INTERFACE RESULT

Figure 4.26 shows the graphical user interface (GUI) layout for detecting the defect of bearing. This figure shows the result for detecting the defect bearing of the data input. Firstly, the user must choose the range of speed running of machine which is 10%, 50% or 90% of the speed of rpm. After that, the reference line will appear in the box of graph. Then, the system will upload the data from the bearing when the load data pushbutton was click. The vibration signal will appear on the graph of signal. FFT pushbutton will function as show the FFT graph of the data.

Then, click the CWT pushbutton for run the decomposition process of the CWT method and also calculating the wavelet coefficient. The scalogram of CWT for the data will show up on the figure. After that, diagnose pushbutton will analysis the wavelet coefficient of data and will make comparison with the reference wavelet coefficient. When the analysis graph shows that the good line bearing is lower from the data line, it shows the bearing was defected. Lastly, the condition of the bearing will be proven either in good condition or not by clicking the condition pushbutton.

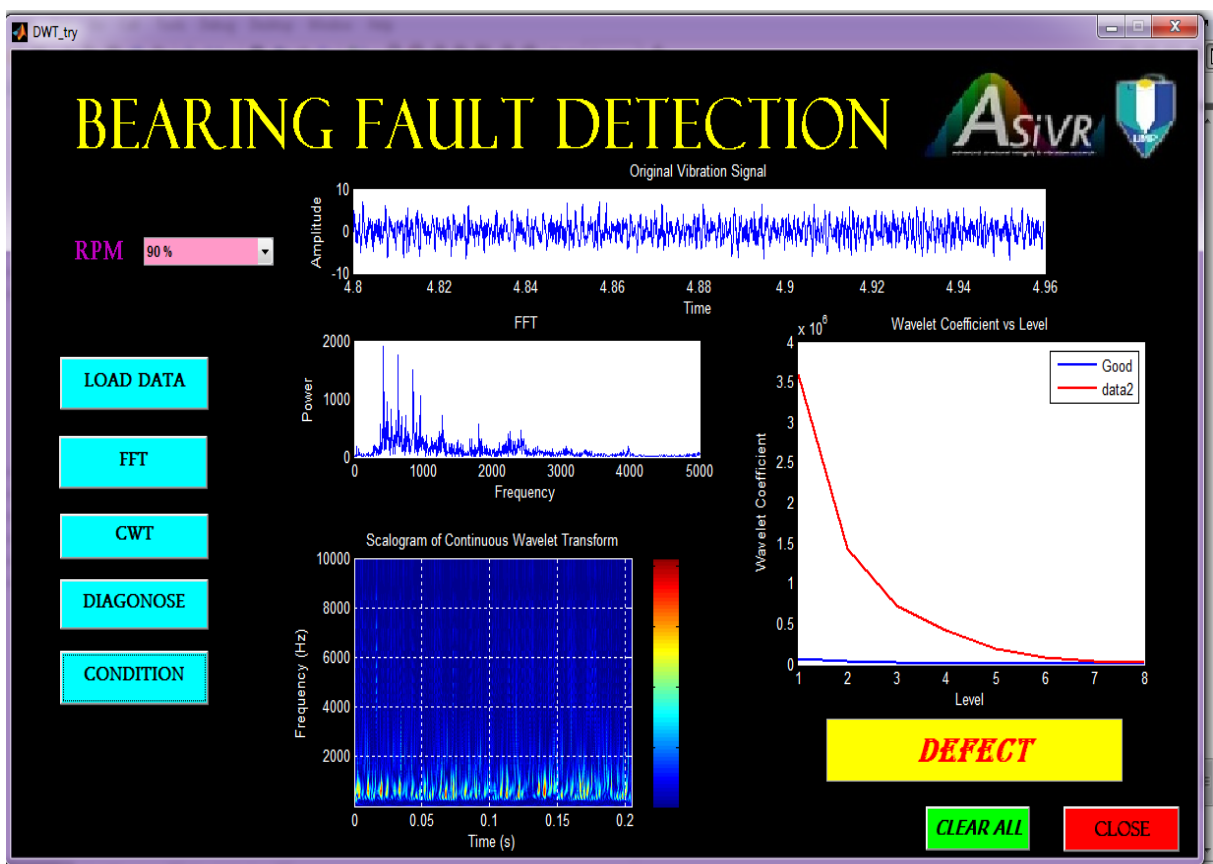


**Figure 4.26:** The result of GUI for defected bearing

While for Figure 4.27 shown the result of GUI for good bearing. When the line of good bearing are upper than the line of data, it will consider the bearing are in good condition. This line is depending on the wavelet coefficient for each level that already calculates from the CWT method process in the CWT pushbutton in the GUI. When

click the clear pushbutton, all the data will be reset and can continue with another data of bearing.

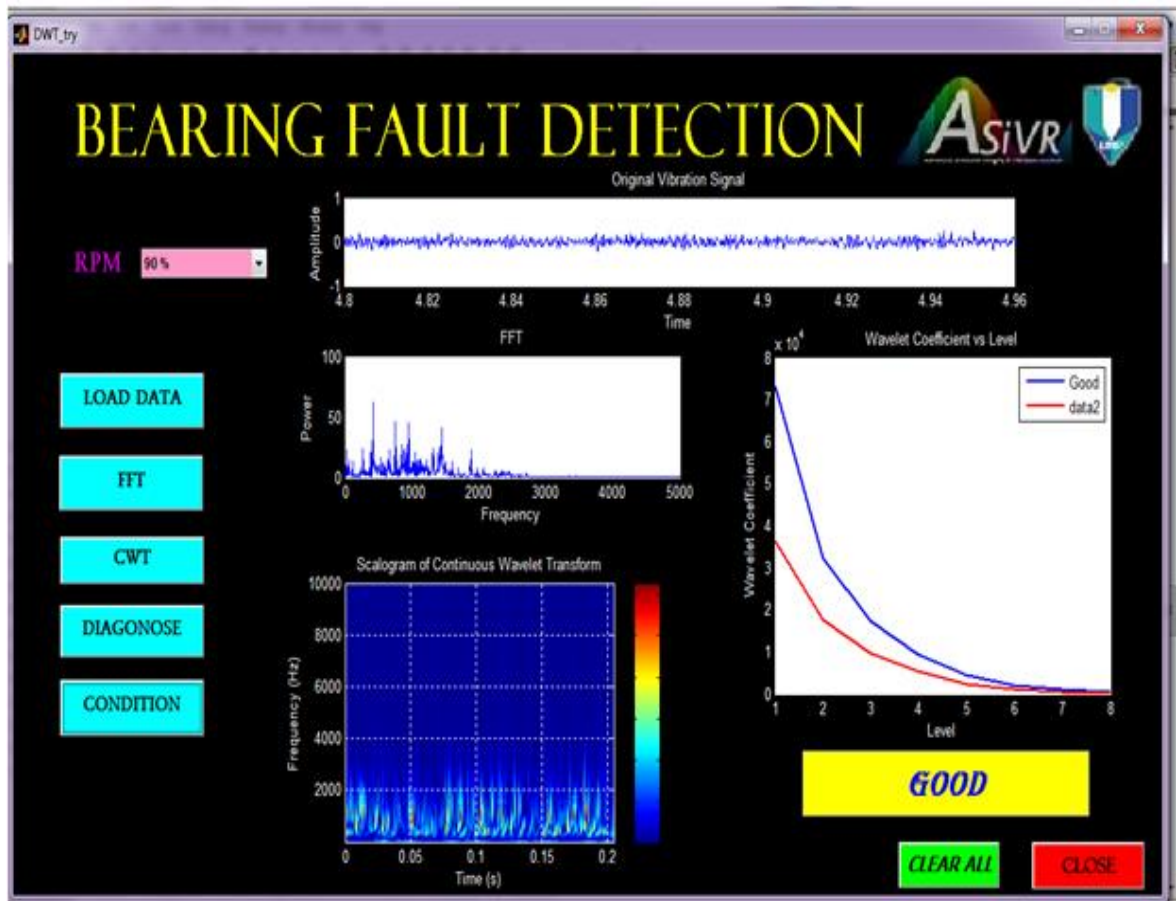


**Figure 4.27:** The result of GUI for bearing in good condition

## CHAPTER 5

### CONCLUSION & RECOMMENDATION

#### 5.1 CONCLUSION

Defect features was successfully detected on all of defective bearings and good condition bearing using Continuous Wavelet Transform (CWT) as they produce vibration signal. Fast Fourier Transform (FFT) and wavelet coefficient plays an important role in supporting result analyzed by using CWT from MATLAB®. Although it is quite hard to differentiate all bearings with time domain, each of the bearing defects and good bearing has their own trend or characteristics when observed. From the analysis, it shows that a system with low operating yields unsystematic result due to low excitation from the defect. For data of insufficient excitation, even though the defect features were weakly observed throughout the decomposition process displays by the scalogram, defect features still may be discovered by calculating and plotting graph for the wavelet coefficient value for each decomposition level. Defected features will show on the wavelet coefficient graph if the wavelet coefficient suddenly decreased at an irregular rate compared to the good bearing. Using CWT is indeed appropriate as an effective tool in detecting defect features in bearing. Clear differentiation of the bearings in any running speed has made it possible for online monitoring without interrupting the machine for checking and maintenance purpose. Therefore, this system is suggested as an alternative technique in bearing fault detection online monitoring.

## 5.2 RECOMMENDATION

For further continuation of this project, many aspect of this project can be improved such as:

- a) Use a different method for analysing the data acquisition.
- b) Detect different types of defect bearing by using GUI software.
- c) Vary kind the defected bearing since there are numbers of types of bearing defect.
- d) Use a wide range of bearing types other than rolling element ball bearings.

## REFERENCES

Al-Ghamd A.M. and Mba D. 2004. A Comparative Experimental Study on the Use of Acoustic Emission and Vibration Analysis for Bearing Defect Identification and Estimation of defect Size. *Mechanical System and Signal Processing* 20:pp.1537-1571.

Braun S., Dartner B., 1997. Analysis of Roller/Ball Bearing Vibration. *ASME Paper 77-WA/DE-5*:pp.1-8

Chen, P.2000. Bearing Condition Monitoring and Fault diagnosis. Msc thesis. University of Calgary, Alberta.

H. Du and S.S. Nair,1998. Identification of friction at low velocities using wavelet basis function network. *Proceedings of the American Control Conference*, pp 1918–1922

H. Zheng, Li, X. Chen. 2002. Gear Fault Diagnosis Based On Continuous Wavelet Transform. *Mechanical Systems and Signal Processing*.pp.447-457

Hans-Georg Stark. 1992. Continuous wavelet transform and continuous multiscale analysis. *Journal of Mathematical Analysis and Applications*.pp. 179-196

J.N. Bradley and C.M. Brislawn, 1994. The wavelet/scalar quantization compression standard for digital fingerprint images. *IEEE Circuits and Systems*, 3:pp.208–208

J.-P. Antoine. 1993. Image analysis with two-dimensional continuous wavelet transform. *Signal Processing (Volume 3)*.pp.241-272

Khalid F, 2007. Rolling element fault diagnosis using Laplace-wavelet envelope power spectrum. *EURASIP Journal on Advances in Signal Processing*.pp.1-4

Kim P.Y., 1984a. A review of rolling element bearing health monitoring (II): Preliminary test results on current technologies. In: *Proceedings of Machinery Vibration Monitoring and Analysis Meeting, Vibration Institute, New Orleans, LA*.26-28 June.pp.127-132

Kim, p.Y. 1984. A Review of Rolling Element Bearing Health Monitorig: Preliminary test Result on Current Proximity Transducer. *Proceedings of 3<sup>rd</sup> International Conference on Vibration in Rotary Machinery*.pp.119-125

L. Debnath. 2001. Wavelet Transforms and Time-Frequency Signal Analysis, Birkhäuser, Boston.

MATLAB, SIMULINK, and Handle Graphics , 1996. Building GUIs with MATLAB Version 5. *The MathWorks, Inc.* pp.1.4-4.3

P. de Groot and L. Deck, 1994. Surface profiling by frequency-domain analysis of white-light interferograms. *Proc. SPIE 2248, Optical measurements and sensors for the process industries.* pp. 101-104

Peng ZK, Chu FL. 2004. Application of the wavelet transform in machine condition monitoring and fault diagnostics: a review with bibliography. *Mech Syst Signal Process.*

R.J.E. Merry, 2005. Wavelet Theory and Applications: A literature study. *Eindhoven*, pp.15-19

Reiz, Zand Lai, M.S. 1989. Detection of Developing Bearing Failures by Means of Vibration. *ASME Design Eng Div DE, 18(1)*:pp.231-6

S. Qian and D. Chen. 1996. Joint Time-Frequency Analysis: Methods and Applications, Prentice-Hall.

SKF, 1994. SKF Handbook: Bearing failures and their causes. *Palmblad Tryckeri AB*. Publication PI 401 E

Tandon N., and A. Choudhury, 1999. A review of vibration and acoustic measurement methods for the detection of defects in rolling element bearing. *Tribology International*. pp.469-480

Volker, E. and Nakra, BC. 1992. Vibration and Acoustic Monitoring Technique for the Detection of Defects in Rolling Element Bearings – A Review. *Shock Vibration digest, 24(3)*:pp.3-11

Wardle, F.P and Poon, S.Y. 1983. Rolling Bearing Noise – cause and Cure. *Chartered Mechanical Engineering*:pp.36-40

## APPENDIX A

## CONTINUOUS WAVELET TRANSFORM MATLAB® CODING

```

function [f,coefs,t]=WaveletAnalysis (Signal,ScaleLength,fs,bs,wavename)
t=[0:bs-1].*(1/fs);
wcf=centfrq(wavename);           % Central frequency of the wavelet
function
cparam=2*wcf*ScaleLength;        % Parameter for calculating the
scales
a=ScaleLength:-1:2;
scal=cparam./a;                  % Scales from which the tranformed
frequencies are arithmetical series
coefs=cwt (Signal,scal,wavename); % Wavelet coefficients
coefsABS=abs (coefs);
f=scal2frq (scal,wavename,1/fs); % Transform the scales to
frequencies

figure(1);
subplot(2,1,1)
plot(t,Signal);
xlabel('Time (s)');
ylabel('Amplitude');
title('Time Domain');
grid on;
subplot (2,1,2)
imagesc(t,f,coefsABS);
shading interp;
axis xy;
xlabel('Time (s)');
ylabel('Frequency (Hz)');
title('Scalogram of continuous wavelet transform');
colorbar;
grid on;

A = xlsread('outer90.xlsx'); % Block30
data=A(122881:126976,2);

```



```

[f,coefs,t]=WaveletAnalysis(data,4097,20000,4096,'db4');

D=abs(sum(coefs(1:4096,:)));           % Calculate coefficient each
level
D1=abs(sum(coefs(1:2047,:)));
D2=abs(sum(coefs(1:1023,:)));
D3=abs(sum(coefs(1:511,:)));
D4=abs(sum(coefs(1:255,:)));
D5=abs(sum(coefs(1:127,:)));
D6=abs(sum(coefs(1:63,:)));
D7=abs(sum(coefs(1:31,:)));
D8=abs(sum(coefs(1:15,:)));

wc1=abs(sum(D1));                    % Calculate sum wavelet coefficient each
level
wc2=abs(sum(D2));
wc3=abs(sum(D3));
wc4=abs(sum(D4));
wc5=abs(sum(D5));
wc6=abs(sum(D6));
wc7=abs(sum(D7));                    x2= (D2);
wc8=abs(sum(D8));                    N2= length (x2);
                                       xsq2= x2.^2;
                                       sumx2= sum (xsq2);
                                       rms2= sqrt (sumx2 / N2);

% Calculate RMS each level
x= (D);
N= length (x);
xsq= x.^2;
sumx= sum (xsq);
rms= sqrt (sumx / N);

x1= (D1);
N1= length (x1);
xsq1= x1.^2;
sumx1= sum (xsq1);
rms1= sqrt (sumx1 / N1);

x2= (D2);
N2= length (x2);
xsq2= x2.^2;
sumx2= sum (xsq2);
rms2= sqrt (sumx2 / N2);

x3= (D3);
N3= length (x3);
xsq3= x3.^2;
sumx3= sum (xsq3);
rms3= sqrt (sumx3 / N3);

x4= (D4);
N4= length (x4);
xsq4= x4.^2;
sumx4= sum (xsq4);
rms4= sqrt (sumx4 / N4);

x5= (D5);
N5= length (x5);

```

```

xsq5= x5.^2;
sumx5= sum (xsq5);
rms5= sqrt (sumx5 / N5);

x6= (D6);
N6= length (x6);
xsq6= x6.^2;
sumx6= sum (xsq6);
rms6= sqrt (sumx6 / N6);
xsq8= x8.^2;
sumx8= sum (xsq8);

% Calculate percentage RMS
for each level decomposition
prms1= (rms1/rms)*100;
prms2= (rms2/rms)*100;
prms3= (rms3/rms)*100;
prms4= (rms4/rms)*100;

x7= (D7);
N7= length (x7);
xsq7= x7.^2;
sumx7= sum (xsq7);
rms7= sqrt (sumx7 / N7);

x8= (D8);
N8= length (x8);
rms8= sqrt (sumx8 / N8);

prms5= (rms5/rms)*100;
prms6= (rms6/rms)*100;
prms7= (rms7/rms)*100;
prms8= (rms8/rms)*100;

% plot fft graph
k=abs(fft(data));

```